Interleukin-13-mediated alterations in esophageal epithelial mitochondria contribute to tissue remodeling in eosinophilic esophagitis

Jazmyne L. Jackson, B.S.[1*], Reshu Saxena, PhD[1*], Mary Grace Murray, B.S.[1*], Abigail J. Staub[2,] Alena Klochkova, MD, PhD[1]. Travis H. Bordner[1], Courtney Worrell[1], Annie D. Fuller, B.S.[1], John M. Crespo, B.S.[1], Andres J. Klein-Szanto, MD, PhD[3], John Elrod, PhD[4], Tatiana A. Karakasheva, PhD[5,6], Melanie Ruffner, MD, PhD[6], Amanda B. Muir, MD[5,6] and Kelly A. Whelan, PhD[1,7]

[1]Fels Cancer Institute for Personalized Medicine, Lewis Katz School of Medicine, Temple University, Philadelphia, PA 19140, USA
[2]Washington and Jefferson College, Washington, PA 15301, USA
[3] Histopathology Facility and Cancer Biology Program, Fox Chase Cancer Center, Philadelphia, PA 19111, USA
[4] Center for Translational Medicine, Lewis Katz School of Medicine at Temple University, Philadelphia, PA 19140, USA
[5]Division of Gastroenterology, Hepatology, and Nutrition, The Children's Hospital of Philadelphia, Philadelphia, PA 19104, USA
[6]Department of Pediatrics, The Children's Hospital of Philadelphia, Philadelphia, PA 19104, USA
[7]Department of Cancer and Cellular Biology, Lewis Katz School of Medicine at Temple University, Philadelphia, PA 19140, USA
*Shared authorship

Correspondence:
Kelly A. Whelan, PhD
Assistant Professor of Cancer & Cellular Biology
Fels Cancer Institute for Personalized Medicine
Temple University Lewis Katz School of Medicine
3307 N. Broad St.
PAHB Room 206
Philadelphia, PA 19140
215-707-8467
kelly.whelan@temple.edu

Conflict of Interest Disclosure: The authors have nothing to disclose.

Funding: This work was supported by the National Institutes of Health: R01DK136987 (KAW), R03AI156435 (KAW), F31DK139760 (JLJ), T32GM142606 (ADF, JMC; PI, Xavier Graña, Johnathan Soboloff), R01GM155497 (THB, CW; PI, Xavier Graña), P30CA006927 (AKS; PI, Jonathan Chernoff). Additionally, support was provided by a Temple University Bridge award, an internal grant provided by the Office of the Vice President for Research (OVPR) at Temple University (KAW).

Abstract

Background: The significance of mitochondria in EoE pathobiology remains elusive.

Objective: To determine the impact of EoE inflammatory mediators upon mitochondrial biology in esophageal epithelium, the mechanisms mediating these effects, and their functional significance to EoE pathobiology.

Methods: Mitochondria were evaluated in human biopsies, MC903/Ovalbumin-induced murine EoE, and human esophageal keratinocytes. Esophageal keratinocytes were treated with EoE-relevant cytokines and JAK/STAT inhibitor ruxolitinib. To deplete mitochondria, 3D organoids generated from *TFAM*$^{loxp/loxp}$ mice were subjected *ex vivo* to Cre or siRNA against Transcription factor A, mitochondria (TFAM) was transfected into esophageal keratinocytes. Mitochondrial respiration, membrane potential, and superoxide levels were measured.

Results: We find evidence of increased mitochondria in esophageal epithelium of patients with EoE and mice with EoE-like inflammation. In esophageal keratinocytes, IL-4 and IL-13 increase mitochondrial mass. IL-13 increases mitochondrial biogenesis in a JAK/STAT-dependent manner. In 3D organoids, IL-13 limits squamous cell differentiation (SCD), and this is blunted upon TFAM depletion. IL-13 decreases mitochondrial respiration and superoxide level, although mitochondria remain intact. IL-13-mediated suppression of superoxide was abrogated upon TFAM depletion in esophageal keratinocytes**.**

Conclusions: We report that increased mitochondrial mass is a feature of EoE. Among EoE-relevant cytokines, IL-13 is the primary driver of increased mitochondrial mass in esophageal keratinocytes by promoting mitochondrial biogenesis in a JAK/STAT-dependent manner. IL-13-mediated accumulation of mitochondria impairs SCD in esophageal keratinocytes and also suppresses oxidative stress, a factor that is known to induce SCD. These findings identify a novel mechanism through which IL-13 promotes EoE-associated epithelial remodeling.

Clinical Implication: These findings further lay a foundation for exploration of level of esophageal epithelial mitochondria as a predictive biomarker for response to dupilumab.

Capsule summary

IL-13 promotes mitochondrial biogenesis in esophageal epithelium, contributing to impaired squamous cell differentiation.

Key Words: Eosinophilic esophagitis; mitochondria; Interleukin-13; squamous differentiation; esophageal epithelium; JAK/STAT signaling

Abbreviations:

ATP: adenosine triphosphate

DHTKD1: dehydrogenase and transketolase domain containing 1

EGD: esophagogastroduodenoscopy

EGID: eosinophilic gastrointestinal diseases

EoE: eosinophilic esophagitis

eos/HPF: eosinophils per high power field

ETC: electron transport chain

FCCP: carbonilcyanide p-triflouromethoxyphenylhydrazone

H&E: hematoxylin & eosin

HIF: hypoxia-inducible factor

IL: Interleukin

IL-4R: IL-4 receptor

KSFM: keratinocyte serum free media

MTCO1: mitochondrially encoded cytochrome c oxidase I

mtDNA: mitochondrial DNA

OCR: oxygen consumption rate

OGDHL: Oxoglutarate dehydrogenase-like

OVA: ovalbumin

OXPHOS: oxidative phosphorylation

ROS: reactive oxygen species

SCD: squamous cell differentiation

siNT: siRNA non-targeting

STAT: signal transducer and activator of transcription

TFAM: transcription factor a, mitochondria

Th: T helper

TNF: Tumor necrosis factor

Introduction

Eosinophilic esophagitis (EoE) is a chronic food allergen- and immune-mediated disease that exerts a significant clinical and financial burden worldwide[1]. EoE is characterized by esophageal eosinophilia and tissue remodeling in esophageal epithelial, muscle, and stromal compartments[1, 2]. EoE symptoms include vomiting, dysphagia and food impaction, all of which negatively impact patient quality of life[3-7]. While dietary elimination and corticosteroids are therapeutic mainstays in EoE, the monoclonal antibody dupilumab, which targets interleukin (IL)-4 receptor (IL-4R)α, became the first and only FDA-approved targeted therapy for use in EoE patients in 2022[8, 9]. This significant advance in EoE patient care was guided by experimental evidence supporting the importance of T helper (Th)2 signaling in EoE. Presently, our understanding of the molecular mechanisms through which Th2 cytokines drive EoE pathobiology remain incompletely understood.

In response to allergens, esophageal epithelial cells secrete cytokines, including thymic stromal lymphopoietin[10, 11], to recruit lymphocytes that then produce Th2 cytokines IL-4, IL-5, and IL-13. In esophageal epithelium, IL-4 and IL-13 bind to IL-4R to promote JAK-mediated phosphorylation of signal transducer and activator of transcription (STAT) proteins[12]. Phosphorylated STATs then dimerize and translocate to the nucleus where they bind DNA and direct target gene transcription[13]. IL-4R-mediated signaling in esophageal epithelium is a key driver of EoE with targeted genetic depletion of epithelial IL-4Rα subunit protecting mice from experimental EoE *in vivo*[14], supporting IL-4R-mediated signaling in esophageal epithelium as a key driver of EoE. Although epithelial-associated IL-4 and IL-13-responsive genes, including eotaxin-3[15, 16], have been linked to EoE pathobiology, studies in mice suggest a predominate role for IL-13 in experimental EoE[14]. We have demonstrated that IL-13 promotes epithelial remodeling, including basal cell accumulation and impaired differentiation, in 3D esophageal organoids[17-19] and these findings have been recapitulated in murine models[14, 20-22]. Additionally, IL-13-mediated induction of calpain-14[23], synaptopodin[24] and follistatin[21] contribute to impaired epithelial squamous cell differentiation (SCD) *in vitro*.

Oxidative stress contributes to regulation of esophageal epithelial differentiation with excessive reactive oxygen species (ROS) promoting SCD[25]. Moreover,

mechanisms that suppress oxidative stress have been linked to EoE-associated epithelial remodeling[18, 21, 26]. For example, our own work has demonstrated that autophagic flux is induced in esophageal keratinocytes responding to IL-13 or tumor necrosis factor (TNF)α to limit oxidative stress[18]. Mitochondria serve as a critical source of cellular ROS, which is produced as a byproduct of oxidative phosphorylation (OXPHOS). Genetic evidence has identified a potential role for mitochondria in the pathogenesis of EoE[27]. Whole exome sequencing on patients with EoE and unaffected family members revealed enrichment in rare, damaging variants in two genes: *DHTKD1 (*Dehydrogenase and Transketolase Domain Containing 1), which contributes to mitochondrial lysine metabolism and ATP production[28, 29], and its homolog *OGDHL (*Oxoglutarate Dehydrogenase-Like)[27]. *In vitro* experiments further revealed significant reductions in mitochondrial respiration in esophageal fibroblasts derived from patients with EoE expressing *DHTKD1* or *OGDHL* variants[27]. Impaired mitochondrial respiration was also identified upon DHTKD1 knockdown in normal esophageal epithelial cultures that further displayed increased levels of ROS[27]. Recently, a study identified evidenced of metabolic dysfunction, including enrichment of OXPHOS pathway, using transcriptomic data from mucosal biopsies of patients with EoE[30].

Here, evaluate the impact of EoE-associated inflammatory mediators upon mitochondrial biology in esophageal epithelium and exploring the mechanisms contributing to these effects and their functional significance in EoE pathobiology.

Methods

Human Subjects

Human subjects were subjected to endoscopic biopsy collection by esophagogastroduodenoscopy (EGD) during routine clinical care under protocols approved by the Institutional Review Board at Hospital of the University of Pennsylvania. At the time of diagnostic esophagogastroduodenoscopy, pinch biopsies were obtained for clinical evaluation. Written informed consent was obtained from each subject or their legal guardian (where appropriate). Patients who met clinical criteria for EoE[31], with mucosal eosinophils per high power field (eos/HPF) were classified as active EoE. Inactive EoE patients had a history of active EoE and clinical showed resolution of esophageal eosinophilia (<15 eos/HPF) at the time of follow up EGD. Normal subjects included those reporting symptoms warranting EGD, but who demonstrated no endoscopic or histological abnormalities in the upper gastrointestinal tract. Subjects with a history of inflammatory bowel disease, celiac disease, GI bleeding or any other acute or chronic intestinal disorders were excluded from recruitment. Demographic and clinical information on human subjects whose esophageal biopsies were evaluated in the current study is provided in **Table E1 in the Online Repository**.

Murine Studies

All animals were purchased, bred, and treated under Temple University Institutional Animal Care and Use Committee-approved protocols. EoE was induced in wild type C57/B6 mice using the MC903/Ovalbumin (OVA) protocol[18, 32] with the following modifications: sensitization period during which MC903 (2 nmol; Tocris Bioscience, Cat# 2700) and OVA (100 μg; Sigma-Aldrich, Cat# A5503-50G) are applied to ears was shortened to from 14 days to 12 days; no treatments were administered on days 13 and 14; OVA in drinking water was increased from 1.5 g/mL to 15 g/mL; challenge period was extended from 4 days to 18 days. Mice treated with MC903 only were used as controls. **Figure E1A in the Online Repository** provides a schematic of the protocol used. B6.Cg-Tfam$^{tm1.1Ncdl}$/J mice (Cat# 026123) were purchased from Jackson Laboratories at age 4-8 weeks. All purchased mice were allowed to acclimate for at least 2 weeks prior to use in experiments. Following experimental protocols, esophagi were harvested and processed as described below.

Immunohistochemistry (IHC) & Histological Evaluation

Formalin-fixed paraffin-embedded tissue section on glass slides were stained with the hematoxylin & eosin (H&E) or the following primary antibodies as previously described[18]: MTCO1 [1D6E1A8] (1:250; Abcam, Cat# ab14705) and TFAM (1:500; Sigma Cat# SAB1401382-50UG). A pathologist blinded to clinical parameters (AKS) scored MTCO1 staining on scale from 0 (negative) to 3, taking into account stain intensity and distribution.

Cell Culture

The immortalized normal esophageal keratinocyte cell line EPC2-hTERT was provided as a generous gift from Drs. Anil Rustgi and Hiroshi Nakagawa (Columbia University). Primary cell cultures generated from esophageal biopsies from a normal human subject (EPC203) and an active EoE patient (EPC128) were provided as a generous gift from Dr. Amanda Muir (CHOP). All cells were cultured in keratinocyte serum free media (KSFM; Gibco, Cat# 17005042) supplemented with recombinant epidermal growth factor (1ng/mL), bovine pituitary extract, (50 μg/mL), and penicillin/streptomycin (1% v/v, Gibco, Cat# 15140-122), as previously described[18]. For experiments with TNFα (R&D Systems, Cat# 210-TA-005/CF; 40 ng/mL), IL-4 (R&D Systems, Cat# 204-IL-010; 10 ng/mL), IL-5 (R&D Systems, Cat# 205-IL-005; 10 ng/mL), IL-13 (R&D Systems, Cat# 213-ILB-005/CF; 10 ng/mL) or IL-1β (R&D Systems, Cat# 201-lB-005; 10 ng/mL), 30,000 cells were plated in 6-well plates, or 100,000 cells were plated on 10-cm plates 24 hours prior to stimulation with cytokines, then media was changed every 48 hours for a total of 7 days. 10 ng/μl stocks of cytokines (20 ng/μl of TNFα) were dissolved in 0.1% Bovine Serum Albumin (Fisher, Cat# BP9703-100) in 1X D-PBS (Gibco, Cat# 14190-144).

To deplete TFAM in esophageal keratinocytes, small interfering RNA oligonucleotides targeting TFAM (Dharmacon, ID: J-019734-06) or a non-targeting (NT) siRNA pool (ID: D-001810-10-05) were diluted in 500 μL Opti-MEM reduced serum media (Gibco, Cat# 31985088) to a final concentration of 10 nM per well of a 6 well tissue culture dish then 5 μL of Lipofectamine™ RNAiMAX transfection reagent

(ThermoFisher Scientific, Cat# 13778150) was added to each well. Plates were incubated at room temperature for 20 minutes then 300,000 EPC2-hTERT cells diluted in 2 mL KSFM without antibiotics were added to each well. 72 hours after siRNA transfection, cells were utilized for experiments.

To suppress the JAK-STAT6 pathway, the JAK inhibitor, Ruxolitinib (100 ng/mL; Invivogen, Cat# tlrl-rux-3) was utilized. The inhibitor was refreshed every 48-72 hours throughout the 7-day period of cytokine stimulation.

Immunoblotting

Whole cell lysates from esophageal keratinocyte cultures or tissue lysates from peeled murine esophageal epithelium were subjected to immunoblotting as described previously[18, 33] using the following primary antibodies: MTCO1 (Abcam, Cat# ab14705, 1:1000), TFAM (Cell Signaling, Cat# 7495, 1:1000), phospho-Stat6 Tyrosine 641 (Cell Signaling, Cat#), STAT6 (Cell Signaling, Cat#), and Actin (Invitrogen, Cat# MA1-744, 1:10000) . Targeted proteins were visualized using chemiluminescence detection reagents (ProSignal Femto ECL Reagent, Cat # 20-302) and imaged on an iBright imaging system (Invitrogen).

Quantitative Polymerase Chain Reaction (qPCR)

For mitochondrial DNA (mtDNA) assays[34], DNA isolation was performed on esophageal keratinocyte cells or peeled murine esophageal epithelium using DNeasy Blood and Tissue Kit (Qiagen, Cat# 69506) according to the manufacturer's instructions. DNA concentration was determined using Qubit™ dsDNA HS Assay Kit according to the manufacturer's instructions (Invitrogen, Cat# Q32851). qPCR was performed using PowerUp™ SYBR™ green master mix (ThermoFisher Scientific, Cat# A25743).

To assess mtDNA, primers for mtDNA D-Loop (murine), *MTCO1* (human) and *ND6* (human) were used. To assess nuclear DNA, primers for *Ikbβ* (murine), *COXIV* (human), and *GAPDH* (human) were used. The relative fold change between the noted mtDNA-encoded genes and nuclear DNA-encoded genes (*Ikbβ* or *GAPDH*) was calculated using the delta delta CT method. In human specimens, the relative

expression of the nuclear DNA-encoded gene *COXIV* was used as an additional internal control.

For reverse transcriptase PCR, RNA extraction was performed with RNeasy Mini Kit (Qiagen, Cat# 74106) according to manufacturer's instructions. RNA concentration was measured using Qubit™ RNA HS Assay Kit (Invitrogen, Cat# Q32852). Reverse transcription was performed using the High-Capacity cDNA Reverse Transcription Kit for RT-qPCR (Thermo Fisher Scientific, Cat# 4368814). qPCR was performed using PowerUp™ SYBR™ green master mix (Thermo Fisher Scientific, Cat# A25743). Primers for *TFAM, MFN1, MFN2, DRP1, PINK1, PARKIN,* and *β-Actin* were used. The relative levels of *TFAM, MFN1, MFN2, DRP1, PINK1,* or *PARKIN* relative to *β*-Actin was calculated using the delta delta CT method. All primer sequences are listed in **Table E2 in the Online Repository**.

Live Cell Imaging

Mitochondria were measured using MitoTracker Green dye (Invitrogen, Cat# M7514). Superoxide level was measured using MitoSOX Red (Invitrogen, Cat# M36008). Esophageal keratinocytes were grown in 100 mm tissue culture plates in the presence or absence of IL-13 (10 ng/mL) for 7 days. On the 6th day, cells were plated on 30 mm glass bottom collagen coated plates overnight then stained with indicated dyes according to the manufacturer's protocol. In brief, cells were stained with KSFM containing 200 nM MitoTracker Green or 5 μM of MitoSOX Red and counterstained with 2 μM of Hoechst (Invitrogen, Cat# 33342), for 30 min at 37°C, 5% CO_2. After staining, cells were washed 3X with HBSS and live cells were analyzed by Leica Confocal Microscope using a 63X oil objective. Cells were maintained at 37°C, 5% CO_2 during imaging. Images were quantified using ImageJ software. Mean integrated intensities of images (from twenty randomly chosen fields) after background subtraction were interpreted as a quantitative measure of mitochondria.

Oxygen Consumption Rate (OCR) Assay

Cellular oxidative phosphorylation (OXPHOS) was monitored using a Seahorse Bioscience Extracellular Flux Analyzer (XF96e, Seahorse Bioscience) by real time OCR

measurement following the protocol of XF Cell Mito Stress Kit (Agilent Technologies, Cat# 103015-100). In brief, EPC2-hTERT cells were grown in 100 mm tissue culture plates with 10 ng/mLIL-13 treatment for 7 days. On the 6th day, 100,000 cells/well were seeded onto XF96 96-well plates in 200 µL of growth medium and incubated overnight at 37 °C, 5% CO_2. One hour prior to assay, culture media was replaced by XF assay media (180 µL; Agilent Technologies, Cat# 102353-100) and cells were incubated at 37°C incubator without CO_2 regulation for 1 hour to allow to pre-equilibration with the XF assay medium which was further supplemented with 25 mM glucose (Sigma, Cat# D8270) and 1 mM sodium pyruvate (pH 7.4; Sigma, Cat# S8636). Cells were sequentially exposed to oligomycin (1 µM), carbonilcyanide p-triflouromethoxyphenylhydrazone (FCCP; 3 µM) and Rotenone plus Antimycin A (1 µM). Basal OCR levels were recorded followed by OCR levels after the injection of individual compounds that inhibit respiratory mitochondrial electron transport chain (ETC) complexes. Results were normalized according to cell protein concentration. Sequential addition of oligomycin, FCCP, as well as rotenone & antimycin A allowed an estimation of the contribution of individual parameters for basal respiration, proton leak, maximal respiration, spare respiratory capacity, non-mitochondrial respiration, and ATP production.

ATP Assay

ATP production was assessed by using the CellTiter-Glo 2.0 Kit (Promega, Cat# G9241) according to the manufacturer's protocol. In brief, EPC2-hTERT cells were grown in 100 mm tissue culture plates in the presence or absence of IL-13 (10 ng/mL) for 7 days. On the 6th day, 100,000 cells/well were seeded onto 96-well solid white plates in 100 µL of growth medium per well and incubated overnight with at 37 °C, 5% CO_2. 100µL of CellTiter-Glo® 2.0 Reagent was added to 100 µl of medium containing cells, followed by mixing for 2 minutes and incubation at room temperature for 10 minutes to stabilize the luminescent signal. Luminescence was measured by using Promega GloMax-Multi+ detection system. Results were expressed as percentage decrease from untreated sample.

Flow cytometry

EPC2-hTERT cells were treated with IL-13 (10 ng/mL) for 7 days with media changes occurring every 48 hours. Mitochondrial membrane potential (depolarized mitochondria) was determined by staining cells with MitoTracker Green (ThermoFisher Scientific, Cat# M7514) at a final concentration of 25 nM and MitoTracker Deep Red (ThermoFisher Scientific, Cat# M22426) at a final concentration of 100 nM. Mitochondrial superoxide production was measured by staining cells with MitoSOX Red (ThermoFisher Scientific, Cat# M36008) at a final concentration of 5 µM. Cells were stained with each dye for 30 minutes at 37°C. Cells were washed with and resuspended in 1X HBSS (Gibco, Cat# 14175095). Flow cytometry was performed using Symphony A5 flow cytometer (BD Biosciences) and data were analyzed with FlowJo version 10.0.

3D Esophageal Organoid Assays

Whole esophagi were dissected from 2 female, 2 male B6.Cg-Tfam tm1.1Ncdl/J mice (age range 12-24 weeks old). Esophageal epithelium was physically separated from underlying submucosa using forceps then the esophagus was cut open longitudinally to expose the epithelial surface. Peeled epithelium was incubated in 1 mL 1X Dispase (Corning, Cat# 354235) in HBSS (Gibco, Cat# 14025-076) for 10 minutes at 37°C with shaking at 1000 RPM. Following removal from Dispase, esophageal epithelium was chopped into 3 pieces with sharp scissors then incubated in 1 mL of 0.25% Trypsin-EDTA (Genesee Scientific, Cat# 25-510) for 10 minutes at 37° C with shaking at 1000 RPM. Trypsin and tissue pieces were forced through a cell strainer (70 µm) into a 50 mL conical tube containing 4 mL of 250µg/mL soybean trypsin inhibitor (Gibco, Cat# 17975-029) in 1X PBS. Cells were pelleted at 1000 RPM for 5 minutes then resuspended in 500 µL of complete 'mouse' KSFM without calcium chloride (Gibco, Cat# 10725-018) supplemented with recombinant epidermal growth factor (1 ng/mL), bovine pituitary extract, (50 mg/mL), and penicillin/streptomycin (1% v/v; Gibco, Cat# 15140-122), and CaCl2 to a final concentration of 0.018 mM (Acros Organics, Cat# 349610025) as previously described[35]. Cell number and viability were measured by Automated Cell Count (Invitrogen, Countess II FL). Single cell suspension in mouse KSFM medium was mixed with 90% Matrigel (Corning, Cat# 354234) to

initiate 3D organoid formation. Using 24 well plates, 4,000 cells were seeded per well in 50 µL Matrigel. After solidification, 500 µL of Advanced DMEM/F12 (Gibco, Cat# 12634-101) supplemented with 1X Glutamax (Gibco, Cat# 35050-061), 1mM HEPES (Gibco, Cat# 15630-080), 1% v/v penicillin-streptomycin (Gibco, Cat# 15140-122), 1X N2 Supplement (Gibco, Cat# 17502-001), 1X B27 Supplement (Gibco, Cat# 17504-044), 0.1 mM N-acetyl-L-cysteine (Fisher Chemical, Cat# 616-91-1), 50 ng/mL human recombinant EGF (Gibco, Cat# 10450-013), 2.0% Noggin/R-Spondin-conditioned media and 10 µM Y27632 (Tocris, Cat# 1254) were added to each well. To initiate recombination, Ad5CMVeGFP virus ($1*10^{11}$pfu/mL; Cat# ad4327) or Ad5CMVCre-eGFP virus ($1*10^{11}$ pfu/mL; Cat# ad4216) purchased from University of Iowa Viral Vector Core was added to growth media at a 1:100 dilution. At the time of plating, organoids were also treated with IL-13 (10 ng/mL) or vehicle. After 48 hours, media was changed to remove virus. Treatment with IL-13 (10 ng/mL) was continued until day 7 with media changes occurring every other day. Organoids were grown for 7 days before recovering from Matrigel with Dispase I and fixing overnight in 4.0% paraformaldehyde. Specimens were embedded in 2.0% Bacto-Agar: 2.5% gelatin prior to paraffin embedding.

EGID Database

To assess the expression of mediators of mitochondrial biology in esophageal biopsies, we accessed the "EoE Transcriptome by RNA Sequencing[36]" section on the EGIDExpress database (https://egidexpress.research.cchmc.org/data/), a site that contains data relating to Eosinophilic Gastrointestinal Diseases (EGIDs).

Statistics

Descriptive statistics are presented as mean ± standard error of the mean (SEM). Student's t-test or one-way analysis of variance was used to determine significance for comparison of two groups. For groups of three or larger, One-way ANOVAs followed by Dunnett's or Tukey's multiple comparisons were performed using GraphPad Prism version 9.0.2 for macOS (GraphPad Software, San Diego, California USA). $p<0.05$ was considered statistically significant.

Results

Evidence of increased mitochondria in esophageal epithelium of EoE patients and mice with EoE-like inflammation

To explore the impact of EoE inflammation upon mitochondria, we evaluated expression of mitochondrial proteins by IHC in human patients with EoE and control subjects with normal esophageal pathology. Staining for MTCO1 (mitochondrially encoded cytochrome c oxidase I), a mitochondrially-encoded subunit of Complex IV of the ETC, was significantly increased in patients with active EoE inflammation as compared to either normal controls or patients with inactive EoE (**Fig. 1A, B**). Increased MTCO1 expression at the protein level was also found in mice with EoE-like inflammation induced by MC903/OVA (**Fig. 2A**), a food allergen-mediated model that exhibits features consistent with EoE pathophysiology as found in humans, including eosinophil-rich inflammatory infiltrates in esophageal mucosa (**see Fig E1A, B in the Online Repository**), impairment of the epithelial proliferation/differentiation gradient, and food impactions[18, 32]. As MTCO1 represents only a single mitochondrial protein, we continued to explore whether EoE inflammation impacts mitochondrial mass. Peeled esophageal epithelium of MC903/OVA-treated mice displayed a significant increase in the ratio of mtDNA relative to nuclear DNA as compared to their MC903-only treated counterparts, the latter of which develop robust atopic dermatitis but fail to exhibit esophageal inflammation (**Fig. 2B**).

IL-13 and IL-4 increase mitochondrial mass in esophageal keratinocytes

We next aimed to define the signals in the EoE inflammatory milieu that promote increased mitochondria in esophageal epithelial cells. To that end, we stimulated the immortalized normal esophageal cell line EPC2-hTERT with a panel of EoE-relevant cytokines, consisting of IL-4, IL-5, IL-13, IL-1β, and TNFα, for 7 days. To assess mitochondria, we performed DNA qPCR for the mitochondrially encoded genes *MTCO1*

and *ND6*. We also evaluated DNA level of *COXIV*, a nuclear gene that encodes the mitochondrial protein cytochrome c oxidase 4. A significant increase in both *MTCO1* and *ND6* was detected in EPC2-hTERT cells treated with IL-4 or IL-13 with the effect induced by IL-13 more pronounced (**Fig. 3A**). EoE-relevant cytokines failed to influence DNA level of *COXIV*, which is expected as EoE has not been shown to induce genetic instability. mtDNA level may result from an increase in mitochondria or an increase in the mtDNA copy number within each mitochondrion. As such, we next used the mitochondrial dye MitoTracker Green to assess mitochondria in IL-13-treated esophageal epithelial cells. Confocal imaging revealed an increase in mitochondria mass along with expansion of the tubular perinuclear mitochondrial network in EPC2-hTERT cells, primary normal, and primary EoE cells treated with IL-13 (**Fig. 3B, C; see Figure E2 in the Online Repository**).

IL-13 and IL-4 promote expression of TFAM in esophageal keratinocytes

An increase in mitochondrial mass may be reflective of increased biogenesis, alterations in fission/fusion dynamics, or impaired mitochondrial turnover, the latter of which primarily occurs via mitophagy[37]. To determine the mechanism through which IL-13 and IL-4 treatment results in accumulation of mitochondria in esophageal keratinocytes, we next used qPCR to survey key genes involved in the regulation of each of these facets of mitochondrial biology. Both IL-13 and IL-4 induced expression of *TFAM*, a critical mediator of biogenesis[38], in EPC2-hTERT cells. The timing of TFAM induction differed with IL-13-stimulated EPC2-hTERT cells showing significant upregulation of *TFAM* at 1, 3, and 7 days of treatment (**Fig. 4A**) while their IL-4-treated counterparts displayed induction at 1 and 5 days of treatment (**see Figure E3A in the Online Repository**). No significant expression of *MFN1* or *MFN2*, encoding critical mediators of mitochondrial fusion Mitofusion1 and Mitofusion2, or in *DRP1,* encoding the critical mediator of mitochondrial fission dynamin-related protein-1 was detected in EPC2-hTERT cells treated with either IL-13 or IL-4 (**Fig. 4B-D; see Figure E3B-D in the Online Repository**). A significant increase in expression of *PINK1* and *PARK2*, encoding mediators of mitophagy PTEN-induced kinase-1 and Parkin, was detected in EPC2-hTERT cells following 5 days of treatment with IL-13 or IL-4 (**Fig. 4E, F**; **see**

Figure E3E, F in the Online Repository). We validated increased levels of TFAM protein in EPC2-hTERT cells treated with IL-13 or IL-4 for 7 days (**Fig. 4G, H**). We further assessed expression of genes involved in mitochondrial biogenesis, fission/fusion, and mitophagy in publicly available transcriptomic data from patients with active EoE and non-EoE controls (EGID database). Expression of T*FAM* was significantly increased in active EoE compared to normal controls[36] (**Fig. 4I**). Additionally, increased levels of MFN1 and MFN2 were detected in active EoE patients which further exhibited diminished levels of *PINK1* and *PARK2*[36] (**Fig. 4I**).

Pharmacological JAK/STAT inhibition limits IL-13-mediated increase in mtDNA and TFAM expression

As IL-13 and IL-4 activate JAK/STAT to promote eosinophilic infiltration and epithelial remodeling in EoE[16], we next aimed to determine if alterations in mitochondrial biology occurring in esophageal epithelia cells responding to IL-13 or IL-4 are dependent upon JAK/STAT signaling. JAK inhibitor ruxolitinib effectively blocked STAT6 phosphorylation at Tyrosine residue 641 (**Fig. 5A**), the site required for STAT6 translocation to the nucleus[39, 40]. Ruxolitinib limited IL-13-mediated increases in both mtDNA and TFAM expression in EPC2-hTERT cells (**Fig. 5A, B**). IL-4-mediated induction of TFAM, however, was not affected by ruxolitinib (**Fig. 5A**).

TFAM depletion limits IL-13-mediated esophageal epithelial remodeling in 3D esophageal organoids

IL-13 is a primary driver of epithelial remodeling in EoE[22, 41, 42]. As such, we next aimed to explore the functional role of IL-13-mediated increase in mitochondria upon esophageal tissue architecture. To do so, we generated 3D esophageal organoids from *Tfam*$^{loxp/loxp}$ mice (**Fig. 6A**). In the absence of Cre-mediated recombination, IL-13 induced a phenotype consistent with BCH, including impaired SCD, along with robust expression of TFAM (**Fig. 6B**). Upon *ex vivo* Cre-mediated recombination, IL-13-treated organoids from *Tfam*$^{loxp/loxp}$ mice displayed effective depletion of TFAM coupled with some evidence of SCD, including decreased basaloid cell content and the presence of centrally-localized keratinized core (**Fig. 6B**).

IL-13 inhibits mitochondrial metabolism without impacting membrane integrity in esophageal keratinocytes

Recently, the bioenergetics in differentiated epithelium were shown to differ from that of undifferentiated epithelium in the esophagus[30]. As IL-13 limits SCD, we continued to examine the influence of IL-13 upon the metabolic profile of esophageal keratinocytes. Seahorse respirometry revealed a decrease in oxygen consumption rate of IL-13-treated EPC2-hTERT cells with suppression of basal, ATP-linked, and maximal respiration (**Fig. 7A-D**). Diminished energy production was further supported as EPC2-hTERT cells and primary esophageal epithelial cultured derived from either a normal non EoE control or patients with active EoE displayed decreases basal ATP levels upon IL-13 stimulation (**Fig. 7E-G**). To determine if decreased mitochondrial respiration is associated with mitochondrial membrane depolarization, we assessed MitoTracker Red (membrane potential sensitive dye) and MitoTracker Red Green (membrane potential insensitive dye) staining in IL-13 treated EPC2-hTERT cells. In these experiments, we found no evidence of alerted levels of mitochondrial depolarization in IL-13-treated cells (**Fig. 7H, I**).

IL-13 suppresses mitochondrial reactive oxygen species, and this effect is blocked by TFAM depletion

Finally, as ROS have been shown to induce SCD in esophageal epithelial cells[21] and mitochondria are a primary source of ROS, we investigated the relationship between IL-13 and oxidative stress in EPC2-hTERT cells. We found that IL-13 limited levels of mitochondrial superoxide in EPC2-hTERT cells (**Fig. 8A, B**). siRNA-mediated TFAM depletion also limited mitochondrial superoxide levels in the absence of IL-13 stimulation (**Fig. 8C, D**); however, when EPC2-hTERT cells were depleted of TFAM, IL-13 treatment failed to limit mitochondrial superoxide levels (**Fig. 8C, D**).

Discussion

While mitochondria have been implicated in various immune-mediated inflammatory pathologies, including asthma and eczema[43, 44], our understanding of the role of this organelle in EoE pathogenesis is limited. We initiated our study by investigating levels of the mitochondrial protein MTCO1 in esophageal biopsy specimens from EoE patients as well as non-EoE controls. We observed a significant increase in the expression of MTCO1, subunit of mitochondrial complex IV, in active EoE patients as compared to either subjects with inactive EoE or controls. We further identified an increase in MTCO1 expression and mtDNA levels in esophageal epithelium of mice with MC903/OVA-induced EoE-like inflammation. In agreement with our findings, a recent report found increased expression of a marker of mitochondrial complex V (ATP synthase) in esophageal epithelium of patients with active EoE[30]. Additionally, although Sherril and colleagues reported decreased levels of DHTKD1 RNA and protein in familial EoE cases, an opposite trend was seen in non-familial EoE cases[27]. Heterogeneity in MTCO1 IHC score was present within each group of human subjects and mice in our datasets. As our *in vitro* studies suggest that IL-13 and IL-4 promote increased mitochondrial mass in esophageal keratinocytes, future investigations will determine if high levels of MTCO1 may be reflective of a subset of EoE patients who are more likely to respond to dupilumab, serving as a predictive biomarker of response. Such investigations will be executed in a prospective and longitudinal fashion, in contrast to the current study in which MTCO1 expression was evaluated retrospectively in a cross-sectional cohort. Notably, metabolic alterations, including activation of the mitochondrial tricarboxylic acid cycle, have been documented in atopic dermatitis patients classified as good responders to dupliumab as compared to poor responders[45]. As mitochondrial dysfunction has been linked to fibrosis in a variety of tissues[46], evaluation of the relationship between mitochondrial mass in esophageal

epithelium and EoE phenotypes in mice and endotypes in human subjects[47] is warranted.

To investigate the influence of EoE inflammatory mediators on mitochondrial mass, we treated esophageal epithelial cells with a panel of EoE-relevant cytokines. Cytokine treatments were performed over 7 days as this was the earliest time point at which reproducible changes in mtDNA content were observed in esophageal epithelial cells *in vitro* (KAW, unpublished data). We found that Th2 cytokines IL-13 and IL-4 significantly increased mitochondrial mass while TNFα significantly decreased mitochondrial mass. As we observed evidence of increased mitochondria in esophageal epithelium of humans and mice with EoE inflammation, the current study investigated the influence of IL-13 and IL-4 on mitochondria in esophageal epithelial cells. However, as the EoE inflammatory milieu is complex, future studies utilizing pharmacologic and/or genetic approaches in murine EoE models will be informative with regard to the inflammatory signals that increase mitochondrial mass in esophageal epithelium *in vivo*. As TNFα is a driver of EoE-associated fibrosis[48-50], it is possible that the balance between IL-13/IL-4 and TNFα and the resulting changes in mitochondrial mass may influence whether EoE presents as inflammatory or fibrotic, which could be tested in murine EoE models. As our own work has demonstrated that aged mice more readily exhibit fibrosis as compared to their young counterparts[51], it will be of interest to examine mitochondrial levels and expression of EoE-relevant cytokines in young and aged mice with EoE-like inflammation. Here, we report that IL-13 and IL-4 induce the expression of TFAM, a critical mediator of mitochondrial biogenesis. As TNFα has been shown to suppress mitochondrial biogenesis concomitant with downregulation of TFAM expression in fat and muscle of obese rodents[52], it is possible that TNFα may inhibit mitochondrial biogenesis in esophageal keratinocytes. Alternatively, TNFα may influence other aspects of mitochondrial biology to decrease mitochondrial mass. We have previously demonstrated that both IL-13 and TNFα promote activation of autophagic flux in esophageal keratinocytes[18]. As mitophagy is a mechanism to clear mitochondria from cells, it is possible that the balance between mitophagy and mitochondrial biogenesis is skewed toward biogenesis in IL-13-treated esophageal keratinocytes while the opposite may be true in cells responding to TNFα.

Our data demonstrate that JAK/STAT signaling contributes to the induction of TFAM in esophageal epithelial cells responding to IL-13. To the best of our knowledge, STAT-mediated transcriptional regulation of TFAM has not been reported. STAT3 has, however, been shown to interact with TFAM at mtDNA, contributing to regulation of mitochondrially-encoded gene expression in murine epidermal keratinocytes[53]. In this context, mitogen signaling phosphorylates STAT3 at Serine 727, permitting STAT3 localization to mitochondria where it interacts with mtDNA and TFAM to limit expression of mitochondrially-encoded genes[53]. While STAT3 depletion augmented mitochondrial respiration in murine epidermal keratinocytes under basal conditions, no effect on mtDNA level was identified[53]. Consistent with this report, we found that pharmacological JAK inhibition had no effect on mtDNA at baseline. We did, however, see that ruxolitinib increased expression of TFAM at the protein level in esophageal keratinocytes in the absence of cytokine stimulation. IL-6-mediated activation of STAT3 has been linked to TFAM downregulation in colonic epithelial cells via microRNA-23b[54]. Thus, there may be multiple mechanisms through which STATs regulate TFAM in a cell-type and/or context-dependent manner. Although recent evidence supports a role for STAT3 in EoE pathogenesis[42], STAT6 is well-established to contribute to EoE pathobiology, including by promoting transcriptional upregulation of eotaxin-3[15, 16, 55], follistatin[21], calpain-14[14, 23, 56], and synaptopodin[24] in esophageal epithelial cells responding to IL-13 or IL-4. Although STAT6 has been shown to translocate to mitochondria and regulate mitochondrial function and fusion in non-epithelial cells[57-60], what role, if any, STAT6 plays in regulation of mitochondrial biology in epithelial cells remains to be determined. STAT1 has also been implicated in EoE[61] and shown to localize to mitochondria and antagonize mitophagy in cardiomyocytes[62]. As we continue to study the regulation of mitochondria by IL-13 and IL-4, we will explore how these Th2 cytokines influence expression and localization (i.e. nucleus vs. mitochondria) of individual STATs as well as the effects of modulating STAT expression, localization, and interactions on mitochondrial biology.

In addition to identifying how the EoE inflammatory milieu influences mitochondrial mass in esophageal epithelium, the current study aimed to investigate the functional role of mitochondria in EoE pathogenesis. Using 3D organoids, we found that

genetic depletion of TFAM partially restored IL-13-mediated impairment of differentiation. As excessive ROS has been shown to induce esophageal epithelial differentiation *in vivo*[21, 25] and mitochondria are a primary source of cellular ROS, we also evaluated the relationship between IL-13, mitochondrial superoxide, and TFAM. In IL-13-treated esophageal epithelial cells, mitochondrial superoxide levels were suppressed. This is consistent with studies showing that although IL-13 initially induces ROS in esophageal epithelium this oxidative stress is alleviated as mechanisms to counteract it are activated, including autophagy and expression of antioxidants[18, 21]. We also find that mitochondrial respiration, which produced ROS as a byproduct, is diminished in IL-13-treated esophageal keratinocytes. It is possible that increased mitochondrial mass occurs as a compensatory mechanism to support energy demands in IL-13-treated cells. Time course experiments will help to clarify the relationship between alterations in mitochondrial mass, respiratory activity, and oxidative stress. The relationship between TFAM and oxidative stress remains ambiguous with some studies showing increased ROS with TFAM knockdown while others demonstrate decreased ROS[63-68]. In EPC2-hTERT cells genetic depletion of TFAM limited mitochondrial superoxide under basal conditions. In contrast, superoxide levels in IL-13-treated esophageal cells were restored upon depletion of TFAM, which also partially restores SCD in IL-13-treated esophageal organoids. The mechanisms underlying the differential effects of TFAM depletion on mitochondrial ROS in esophageal keratinocytes in the presence and absence of IL-13 remain to be determined.

One final consideration is examination of how IL-13-mediated increase in mitochondrial mass in esophageal keratinocytes may relate to proliferation, which is coupled with SCD in esophageal epithelium wherein proliferative basal/suprabasal cells exit the cell cycle as they differentiate. Diminished reliance on mitochondrial metabolism is a feature of many dividing mammalian cells that preferentially use glycolysis for energy production as it increases availability of carbon and other resources that are needed to increase biomass[69]. Although this concept provides rationale to support diminished mitochondrial activity in IL-13-treated esophageal keratinocytes, it also operates under the assumption that IL-13 drives proliferation in this context. The reality may be more complex. In EPC2-hTERT cells, heterogeneity was

recently identified with regard to proliferation as clonal tracing revealed that only ~10% of clones exhibit exponential growth in non-genetic heritable fashion[70]. Thus, effects on mitochondria and cell metabolism mediated by EoE-relevant cytokines may represent behaviors attributable to subsets of cells, which could be explored using single-cell based approaches. Evaluation of cellular heterogeneity in esophageal epithelium and in response to inflammatory stress may also help to reconcile our findings with a recent study indicating that enhanced mitochondrial activity is associated with impaired differentiation in esophageal epithelium[30]. In the study by Ryan et al, dysregulated hypoxia-inducible factor (HIF)-1α signaling enhances mitochondrial respiration and diminishes glycolysis which is associated with impaired calcium-induced differentiation *in vitro*[30]. In macrophages, HIF-1α-mediated induction of glycolysis has been shown to promote classical pro-inflammatory activation, while IL-4-mediated induction of STAT6 and mitochondrial biogenesis supports alternative anti-inflammatory activation. These findings supporting the premise that integration of cell signaling and metabolism may influence specific cell fate decisions in a cell population. With regard to the role of proliferation in EoE-associated epithelial remodeling, biopsies from patients with active EoE exhibit an increase in both SOX2-postive and KI67-positive cells; however, no significant difference in proliferative (Ki67-positive) basal (SOX2-poitive) cells was found in these subjects[17]. In both EoE patients and mice with MC903/OVA-mediated EoE-like inflammation, reported evidence of suprabasal cell expansion has been reported[71, 72], indicating that BCH in EoE may be linked to factors beyond an increase in basal cell proliferation. Supabasal cell expansion was also identified in human subjects with EoE[72]. In mice, EoE-associated suprabasal cells exhibited evidence of senescence[71], a pathway that is linked to mitochondrial ROS production. In salivary epithelial cells, STAT6 signaling has been linked to mitochondrial dysfunction and ROS production that drives senescence[59].

In conclusion, we utilized human and murine esophageal tissue with EoE inflammation as well as *in vitro* and *ex vivo* models to delineate the role of mitochondria in EoE pathogenesis. Specifically, IL-13 promotes increased intracellular mitochondria within the esophageal epithelium which in turn contributes to impaired squamous differentiation. Moreover, diminished ROS in response to IL-13, a known regulator of

differentiation, is supported by increased mitochondrial biogenesis. We propose a model wherein IL-13-mediated STAT signaling promotes expression of TFAM and accumulation of mitochondria with diminished respiratory activity, providing a limited supply of ROS to induce SCD. Thus, these findings provide novel insights into the underlying mechanisms through which EoE inflammatory mediators influence mitochondrial biology as well as the functional role of mitochondria in EoE pathogenesis.

Acknowledgments: We thank the following former members of the Whelan lab for their support Anbin Mu, Timothy Hall, Anne-Laure Monéger, Julie Gang, and M. Faujul Kabir. We acknowledge the staff of following core facilities for technical assistance: Temple University Lewis Katz School of Medicine Flow Cytometry Core, (Director, Amir Yarmahoodi); Fox Chase Cancer Center Histopathology Core; Children's Hospital of Philadelphia Gastrointestinal Epithelium Modeling Program Core (RRID: SCR_026402) and the University of Pennsylvania Center for Molecular Studies in Digestive and Liver Diseases (NIHP30DK050306).

References

1. Muir A, Falk GW. Eosinophilic Esophagitis: A Review. JAMA. 2021;326(13):1310-8. doi: 10.1001/jama.2021.14920. PubMed PMID: 34609446; PMCID: PMC9045493.

2. Dellon ES, Liacouras CA, Molina-Infante J, Furuta GT, Spergel JM, Zevit N, Spechler SJ, Attwood SE, Straumann A, Aceves SS, Alexander JA, Atkins D, Arva NC, Blanchard C, Bonis PA, Book WM, Capocelli KE, Chehade M, Cheng E, Collins MH, Davis CM, Dias JA, Di Lorenzo C, Dohil R, Dupont C, Falk GW, Ferreira CT, Fox A, Gonsalves NP, Gupta SK, Katzka DA, Kinoshita Y, Menard-Katcher C, Kodroff E, Metz DC, Miehlke S, Muir AB, Mukkada VA, Murch S, Nurko S, Ohtsuka Y, Orel R, Papadopoulou A, Peterson KA, Philpott H, Putnam PE, Richter JE, Rosen R, Rothenberg ME, Schoepfer A, Scott MM, Shah N, Sheikh J, Souza RF, Strobel MJ, Talley NJ, Vaezi MF, Vandenplas Y, Vieira MC, Walker MM, Wechsler JB, Wershil BK, Wen T, Yang GY, Hirano I, Bredenoord AJ. Updated International Consensus Diagnostic Criteria for Eosinophilic Esophagitis: Proceedings of the AGREE Conference. Gastroenterology. 2018;155(4):1022-33.e10. Epub 20180906. doi: 10.1053/j.gastro.2018.07.009. PubMed PMID: 30009819; PMCID: PMC6174113.

3. Thel HL, Anderson C, Xue AZ, Jensen ET, Dellon ES. Prevalence and Costs of Eosinophilic Esophagitis in the United States. Clin Gastroenterol Hepatol. 2024. Epub 20241031. doi: 10.1016/j.cgh.2024.09.031. PubMed PMID: 39486752.

4. Chehade M, Hiremath GS, Zevit N, Oliva S, Pela T, Khodzhayev A, Jacob-Nara J, Radwan A. Disease Burden and Spectrum of Symptoms that Impact Quality of Life in Pediatric Patients with Eosinophilic Esophagitis. Gastro Hep Adv. 2024;3(8):1054-68. Epub 20240822. doi: 10.1016/j.gastha.2024.08.009. PubMed PMID: 39529644; PMCID: PMC11550740.

5. Liacouras CA, Furuta GT, Hirano I, Atkins D, Attwood SE, Bonis PA, Burks AW, Chehade M, Collins MH, Dellon ES, Dohil R, Falk GW, Gonsalves N, Gupta SK, Katzka DA, Lucendo AJ, Markowitz JE, Noel RJ, Odze RD, Putnam PE, Richter JE, Romero Y, Ruchelli E, Sampson HA, Schoepfer A, Shaheen NJ, Sicherer SH, Spechler S, Spergel JM, Straumann A, Wershil BK, Rothenberg ME, Aceves SS. Eosinophilic esophagitis: updated consensus recommendations for children and adults. J Allergy Clin Immunol. 2011;128(1):3-20 e6; quiz 1-2. Epub 2011/04/12. doi: 10.1016/j.jaci.2011.02.040. PubMed PMID: 21477849.

6. Furuta GT, Katzka DA. Eosinophilic Esophagitis. N Engl J Med. 2015;373(17):1640-8. Epub 2015/10/22. doi: 10.1056/NEJMra1502863. PubMed PMID: 26488694; PMCID: PMC4905697.
7. Klinnert MD. Psychological impact of eosinophilic esophagitis on children and families. Immunol Allergy Clin North Am. 2009;29(1):99-107, x. doi: 10.1016/j.iac.2008.09.011. PubMed PMID: 19141345.
8. Hirano I, Dellon ES, Hamilton JD, Collins MH, Peterson K, Chehade M, Schoepfer AM, Safroneeva E, Rothenberg ME, Falk GW, Assouline-Dayan Y, Zhao Q, Chen Z, Swanson BN, Pirozzi G, Mannent L, Graham NMH, Akinlade B, Stahl N, Yancopoulos GD, Radin A. Efficacy of Dupilumab in a Phase 2 Randomized Trial of Adults With Active Eosinophilic Esophagitis. Gastroenterology. 2020;158(1):111-22.e10. Epub 20191005. doi: 10.1053/j.gastro.2019.09.042. PubMed PMID: 31593702.
9. Harb H, Chatila TA. Mechanisms of Dupilumab. Clin Exp Allergy. 2020;50(1):5-14. Epub 20190930. doi: 10.1111/cea.13491. PubMed PMID: 31505066; PMCID: PMC6930967.
10. Chandramouleeswaran PM, Shen D, Lee AJ, Benitez A, Dods K, Gambanga F, Wilkins BJ, Merves J, Noah Y, Toltzis S, Yearley JH, Spergel JM, Nakagawa H, Malefyt R, Muir AB, Wang ML. Preferential Secretion of Thymic Stromal Lymphopoietin (TSLP) by Terminally Differentiated Esophageal Epithelial Cells: Relevance to Eosinophilic Esophagitis (EoE). PLoS One. 2016;11(3):e0150968. Epub 20160318. doi: 10.1371/journal.pone.0150968. PubMed PMID: 26992000; PMCID: PMC4798725.
11. Rothenberg ME, Spergel JM, Sherrill JD, Annaiah K, Martin LJ, Cianferoni A, Gober L, Kim C, Glessner J, Frackelton E, Thomas K, Blanchard C, Liacouras C, Verma R, Aceves S, Collins MH, Brown-Whitehorn T, Putnam PE, Franciosi JP, Chiavacci RM, Grant SF, Abonia JP, Sleiman PM, Hakonarson H. Common variants at 5q22 associate with pediatric eosinophilic esophagitis. Nat Genet. 2010;42(4):289-91. Epub 20100307. doi: 10.1038/ng.547. PubMed PMID: 20208534; PMCID: PMC3740732.
12. Jiang H, Harris MB, Rothman P. IL-4/IL-13 signaling beyond JAK/STAT. J Allergy Clin Immunol. 2000;105(6 Pt 1):1063-70. doi: 10.1067/mai.2000.107604. PubMed PMID: 10856136.
13. Hershey GK. IL-13 receptors and signaling pathways: an evolving web. J Allergy Clin Immunol. 2003;111(4):677-90; quiz 91. doi: 10.1067/mai.2003.1333. PubMed PMID: 12704343.
14. Avlas S, Shani G, Rhone N, Itan M, Dolitzky A, Hazut I, Grisaru-Tal S, Gordon Y, Shoda T, Ballaban A, Ben-Baruch NM, Rochman M, Diesendruck Y, Nahary L, Bitton A, Halpern Z, Benhar I, Varol C, Rothenberg ME, Munitz A. Epithelial cell-expressed type II IL-4 receptor mediates eosinophilic esophagitis. Allergy. 2022. Epub 20220907. doi: 10.1111/all.15510. PubMed PMID: 36070083.
15. Blanchard C, Wang N, Stringer KF, Mishra A, Fulkerson PC, Abonia JP, Jameson SC, Kirby C, Konikoff MR, Collins MH, Cohen MB, Akers R, Hogan SP, Assa'ad AH, Putnam PE, Aronow BJ, Rothenberg ME. Eotaxin-3 and a uniquely conserved gene-expression profile in eosinophilic esophagitis. J Clin Invest. 2006;116(2):536-47. doi: 10.1172/JCI26679. PubMed PMID: 16453027; PMCID: PMC1359059.
16. Cheng E, Zhang X, Wilson KS, Wang DH, Park JY, Huo X, Yu C, Zhang Q, Spechler SJ, Souza RF. JAK-STAT6 Pathway Inhibitors Block Eotaxin-3 Secretion by Epithelial Cells and Fibroblasts from Esophageal Eosinophilia Patients: Promising

Agents to Improve Inflammation and Prevent Fibrosis in EoE. PLoS One. 2016;11(6):e0157376. Epub 20160616. doi: 10.1371/journal.pone.0157376. PubMed PMID: 27310888; PMCID: PMC4911010.

17. Hara T, Kasagi Y, Wang J, Sasaki M, Aaron B, Karami A, Shimonosono M, Shimonosono R, Maekawa H, Dolinsky L, Wilkins B, Klein J, Wei J, Nunes K, Lynch K, Spergel JM, Hamilton KE, Ruffner MA, Karakasheva TA, Whelan KA, Nakagawa H, Muir AB. CD73. Cell Mol Gastroenterol Hepatol. 2022;13(5):1449-67. Epub 20220130. doi: 10.1016/j.jcmgh.2022.01.018. PubMed PMID: 35108658; PMCID: PMC8957025.

18. Whelan KA, Merves JF, Giroux V, Tanaka K, Guo A, Chandramouleeswaran PM, Benitez AJ, Dods K, Que J, Masterson JC, Fernando SD, Godwin BC, Klein-Szanto AJ, Chikwava K, Ruchelli ED, Hamilton KE, Muir AB, Wang ML, Furuta GT, Falk GW, Spergel JM, Nakagawa H. Autophagy mediates epithelial cytoprotection in eosinophilic oesophagitis. Gut. 2017;66(7):1197-207. Epub 20160216. doi: 10.1136/gutjnl-2015-310341. PubMed PMID: 26884425; PMCID: PMC4987278.

19. Kasagi Y, Chandramouleeswaran PM, Whelan KA, Tanaka K, Giroux V, Sharma M, Wang J, Benitez AJ, DeMarshall M, Tobias JW, Hamilton KE, Falk GW, Spergel JM, Klein-Szanto AJ, Rustgi AK, Muir AB, Nakagawa H. The Esophageal Organoid System Reveals Functional Interplay Between Notch and Cytokines in Reactive Epithelial Changes. Cell Mol Gastroenterol Hepatol. 2018;5(3):333-52. Epub 20180103. doi: 10.1016/j.jcmgh.2017.12.013. PubMed PMID: 29552622; PMCID: PMC5852293.

20. Mishra A, Rothenberg ME. Intratracheal IL-13 induces eosinophilic esophagitis by an IL-5, eotaxin-1, and STAT6-dependent mechanism. Gastroenterology. 2003;125(5):1419-27. doi: 10.1016/j.gastro.2003.07.007. PubMed PMID: 14598258.

21. Jiang M, Ku WY, Zhou Z, Dellon ES, Falk GW, Nakagawa H, Wang ML, Liu K, Wang J, Katzka DA, Peters JH, Lan X, Que J. BMP-driven NRF2 activation in esophageal basal cell differentiation and eosinophilic esophagitis. J Clin Invest. 2015;125(4):1557-68. Epub 2015/03/17. doi: 10.1172/JCI78850. PubMed PMID: 25774506; PMCID: PMC4396468.

22. Zuo L, Fulkerson PC, Finkelman FD, Mingler M, Fischetti CA, Blanchard C, Rothenberg ME. IL-13 induces esophageal remodeling and gene expression by an eosinophil-independent, IL-13R alpha 2-inhibited pathway. J Immunol. 2010;185(1):660-9. Epub 20100611. doi: 10.4049/jimmunol.1000471. PubMed PMID: 20543112; PMCID: PMC3746758.

23. Davis BP, Stucke EM, Khorki ME, Litosh VA, Rymer JK, Rochman M, Travers J, Kottyan LC, Rothenberg ME. Eosinophilic esophagitis-linked calpain 14 is an IL-13-induced protease that mediates esophageal epithelial barrier impairment. JCI Insight. 2016;1(4):e86355. doi: 10.1172/jci.insight.86355. PubMed PMID: 27158675; PMCID: PMC4855700.

24. Rochman M, Travers J, Abonia JP, Caldwell JM, Rothenberg ME. Synaptopodin is upregulated by IL-13 in eosinophilic esophagitis and regulates esophageal epithelial cell motility and barrier integrity. JCI Insight. 2017;2(20). Epub 20171019. doi: 10.1172/jci.insight.96789. PubMed PMID: 29046486; PMCID: PMC5846900.

25. Chen H, Hu Y, Fang Y, Djukic Z, Yamamoto M, Shaheen NJ, Orlando RC, Chen X. Nrf2 deficiency impairs the barrier function of mouse oesophageal epithelium. Gut. 2014;63(5):711-9. Epub 20130515. doi: 10.1136/gutjnl-2012-303731. PubMed PMID: 23676441; PMCID: PMC3883925.

26. Hishida T, Vazquez-Ferrer E, Hishida-Nozaki Y, Takemoto Y, Hatanaka F, Yoshida K, Prieto J, Sahu SK, Takahashi Y, Reddy P, O'Keefe DD, Rodriguez Esteban C, Knoepfler PS, Nuñez Delicado E, Castells A, Campistol JM, Kato R, Nakagawa H, Izpisua Belmonte JC. Myc Supports Self-Renewal of Basal Cells in the Esophageal Epithelium. Front Cell Dev Biol. 2022;10:786031. Epub 20220304. doi: 10.3389/fcell.2022.786031. PubMed PMID: 35309931; PMCID: PMC8931341.
27. Sherrill JD, Kc K, Wang X, Wen T, Chamberlin A, Stucke EM, Collins MH, Abonia JP, Peng Y, Wu Q, Putnam PE, Dexheimer PJ, Aronow BJ, Kottyan LC, Kaufman KM, Harley JB, Huang T, Rothenberg ME. Whole-exome sequencing uncovers oxidoreductases DHTKD1 and OGDHL as linkers between mitochondrial dysfunction and eosinophilic esophagitis. JCI Insight. 2018;3(8). Epub 20180419. doi: 10.1172/jci.insight.99922. PubMed PMID: 29669943; PMCID: PMC5931135.
28. Danhauser K, Sauer SW, Haack TB, Wieland T, Staufner C, Graf E, Zschocke J, Strom TM, Traub T, Okun JG, Meitinger T, Hoffmann GF, Prokisch H, Kölker S. DHTKD1 mutations cause 2-aminoadipic and 2-oxoadipic aciduria. Am J Hum Genet. 2012;91(6):1082-7. Epub 20121108. doi: 10.1016/j.ajhg.2012.10.006. PubMed PMID: 23141293; PMCID: PMC3516599.
29. Xu W, Zhu H, Gu M, Luo Q, Ding J, Yao Y, Chen F, Wang Z. DHTKD1 is essential for mitochondrial biogenesis and function maintenance. FEBS Lett. 2013;587(21):3587-92. Epub 20130927. doi: 10.1016/j.febslet.2013.08.047. PubMed PMID: 24076469.
30. Ryan S, Crowe L, Almeida Cruz SN, Galbraith MD, O'Brien C, Hammer JA, Bergin R, Kellett SK, Markey GE, Benson TM, Fagan O, Espinosa JM, Conlon N, Donohoe CL, McKiernan S, Hogan AE, McNamee EN, Furuta GT, Menard-Katcher C, Masterson JC. Metabolic dysfunction mediated by HIF-1α contributes to epithelial differentiation defects in eosinophilic esophagitis. J Allergy Clin Immunol. 2024;154(6):1472-88. Epub 20240827. doi: 10.1016/j.jaci.2024.07.030. PubMed PMID: 39209164.
31. Dellon ES. Eosinophilic esophagitis: diagnostic tests and criteria. Curr Opin Gastroenterol. 2012;28(4):382-8. Epub 2012/03/28. doi: 10.1097/MOG.0b013e328352b5ef. PubMed PMID: 22450900; PMCID: PMC4591255.
32. Noti M, Wojno ED, Kim BS, Siracusa MC, Giacomin PR, Nair MG, Benitez AJ, Ruymann KR, Muir AB, Hill DA, Chikwava KR, Moghaddam AE, Sattentau QJ, Alex A, Zhou C, Yearley JH, Menard-Katcher P, Kubo M, Obata-Ninomiya K, Karasuyama H, Comeau MR, Brown-Whitehorn T, de Waal Malefyt R, Sleiman PM, Hakonarson H, Cianferoni A, Falk GW, Wang ML, Spergel JM, Artis D. Thymic stromal lymphopoietin-elicited basophil responses promote eosinophilic esophagitis. Nat Med. 2013;19(8):1005-13. Epub 2013/07/23. doi: 10.1038/nm.3281. PubMed PMID: 23872715; PMCID: PMC3951204.
33. Natsuizaka M, Whelan KA, Kagawa S, Tanaka K, Giroux V, Chandramouleeswaran PM, Long A, Sahu V, Darling DS, Que J, Yang Y, Katz JP, Wileyto EP, Basu D, Kita Y, Natsugoe S, Naganuma S, Klein-Szanto AJ, Diehl JA, Bass AJ, Wong KK, Rustgi AK, Nakagawa H. Interplay between Notch1 and Notch3 promotes EMT and tumor initiation in squamous cell carcinoma. Nat Commun. 2017;8(1):1758. Epub 2017/11/25. doi: 10.1038/s41467-017-01500-9. PubMed PMID: 29170450; PMCID: PMC5700926.

34. Whelan KA, Chandramouleeswaran PM, Tanaka K, Natsuizaka M, Guha M, Srinivasan S, Darling DS, Kita Y, Natsugoe S, Winkler JD, Klein-Szanto AJ, Amaravadi RK, Avadhani NG, Rustgi AK, Nakagawa H. Autophagy supports generation of cells with high CD44 expression via modulation of oxidative stress and Parkin-mediated mitochondrial clearance. Oncogene. 2017;36(34):4843-58. Epub 2017/04/18. doi: 10.1038/onc.2017.102. PubMed PMID: 28414310; PMCID: PMC5570661.
35. Kabir MF, Karami AL, Cruz-Acuña R, Klochkova A, Saxena R, Mu A, Murray MG, Cruz J, Fuller AD, Clevenger MH, Chitrala KN, Tan Y, Keith K, Madzo J, Huang H, Jelinek J, Karakasheva T, Hamilton KE, Muir AB, Tétreault MP, Whelan KA. Single cell transcriptomic analysis reveals cellular diversity of murine esophageal epithelium. Nat Commun. 2022;13(1):2167. Epub 20220420. doi: 10.1038/s41467-022-29747-x. PubMed PMID: 35443762; PMCID: PMC9021266.
36. Sherrill JD, Kiran KC, Blanchard C, Stucke EM, Kemme KA, Collins MH, Abonia JP, Putnam PE, Mukkada VA, Kaul A, Kocoshis SA, Kushner JP, Plassard AJ, Karns RA, Dexheimer PJ, Aronow BJ, Rothenberg ME. Analysis and expansion of the eosinophilic esophagitis transcriptome by RNA sequencing. Genes Immun. 2014;15(6):361-9. Epub 20140612. doi: 10.1038/gene.2014.27. PubMed PMID: 24920534; PMCID: PMC4156528.
37. Youle RJ, van der Bliek AM. Mitochondrial fission, fusion, and stress. Science. 2012;337(6098):1062-5. doi: 10.1126/science.1219855. PubMed PMID: 22936770; PMCID: PMC4762028.
38. Picca A, Lezza AM. Regulation of mitochondrial biogenesis through TFAM-mitochondrial DNA interactions: Useful insights from aging and calorie restriction studies. Mitochondrion. 2015;25:67-75. Epub 20151003. doi: 10.1016/j.mito.2015.10.001. PubMed PMID: 26437364.
39. Mikita T, Campbell D, Wu P, Williamson K, Schindler U. Requirements for interleukin-4-induced gene expression and functional characterization of Stat6. Mol Cell Biol. 1996;16(10):5811-20. doi: 10.1128/MCB.16.10.5811. PubMed PMID: 8816495; PMCID: PMC231582.
40. Pesu M, Takaluoma K, Aittomäki S, Lagerstedt A, Saksela K, Kovanen PE, Silvennoinen O. Interleukin-4-induced transcriptional activation by stat6 involves multiple serine/threonine kinase pathways and serine phosphorylation of stat6. Blood. 2000;95(2):494-502. PubMed PMID: 10627454.
41. Mavi P, Rajavelu P, Rayapudi M, Paul RJ, Mishra A. Esophageal functional impairments in experimental eosinophilic esophagitis. Am J Physiol Gastrointest Liver Physiol. 2012;302(11):G1347-55. Epub 20120223. doi: 10.1152/ajpgi.00013.2012. PubMed PMID: 22361731; PMCID: PMC3378164.
42. Marella S, Sharma A, Ganesan V, Ferrer-Torres D, Krempski JW, Idelman G, Clark S, Nasiri Z, Vanoni S, Zeng C, Dlugosz AA, Zhou H, Wang S, Doyle AD, Wright BL, Spence JR, Chehade M, Hogan SP. IL-13-induced STAT3-dependent signaling networks regulate esophageal epithelial proliferation in eosinophilic esophagitis. J Allergy Clin Immunol. 2023;152(6):1550-68. Epub 20230829. doi: 10.1016/j.jaci.2023.07.021. PubMed PMID: 37652141; PMCID: PMC11102758.
43. Reddy PH. Mitochondrial Dysfunction and Oxidative Stress in Asthma: Implications for Mitochondria-Targeted Antioxidant Therapeutics. Pharmaceuticals

(Basel). 2011;4(3):429-56. doi: 10.3390/ph4030429. PubMed PMID: 21461182; PMCID: PMC3066010.

44. Sreedhar A, Aguilera-Aguirre L, Singh KK. Mitochondria in skin health, aging, and disease. Cell Death Dis. 2020;11(6):444. Epub 20200609. doi: 10.1038/s41419-020-2649-z. PubMed PMID: 32518230; PMCID: PMC7283348.

45. Zhang L, Wen X, Hou Y, Yang Y, Song W, Zeng Y, Sun J. Integrated metabolomics and lipidomics study of patients with atopic dermatitis in response to dupilumab. Front Immunol. 2022;13:1002536. Epub 20221020. doi: 10.3389/fimmu.2022.1002536. PubMed PMID: 36341398; PMCID: PMC9632449.

46. Li X, Zhang W, Cao Q, Wang Z, Zhao M, Xu L, Zhuang Q. Mitochondrial dysfunction in fibrotic diseases. Cell Death Discov. 2020;6:80. Epub 20200905. doi: 10.1038/s41420-020-00316-9. PubMed PMID: 32963808; PMCID: PMC7474731.

47. Shoda T, Wen T, Aceves SS, Abonia JP, Atkins D, Bonis PA, Caldwell JM, Capocelli KE, Carpenter CL, Collins MH, Dellon ES, Eby MD, Gonsalves N, Gupta SK, Falk GW, Hirano I, Menard-Katcher P, Kuhl JT, Krischer JP, Leung J, Mukkada VA, Spergel JM, Trimarchi MP, Yang GY, Zimmermann N, Furuta GT, Rothenberg ME, (CEGIR) CoEGDR. Eosinophilic oesophagitis endotype classification by molecular, clinical, and histopathological analyses: a cross-sectional study. Lancet Gastroenterol Hepatol. 2018;3(7):477-88. Epub 20180503. doi: 10.1016/S2468-1253(18)30096-7. PubMed PMID: 29730081; PMCID: PMC5997568.

48. Muir AB, Karakasheva TA, Whelan KA. Epithelial-Fibroblast Crosstalk in Eosinophilic Esophagitis. Cell Mol Gastroenterol Hepatol. 2024;17(5):713-8. Epub 20240203. doi: 10.1016/j.jcmgh.2024.01.020. PubMed PMID: 38316214; PMCID: PMC10957450.

49. Kasagi Y, Dods K, Wang JX, Chandramouleeswaran PM, Benitez AJ, Gambanga F, Kluger J, Ashorobi T, Gross J, Tobias JW, Klein-Szanto AJ, Spergel JM, Cianferoni A, Falk GW, Whelan KA, Nakagawa H, Muir AB. Fibrostenotic eosinophilic esophagitis might reflect epithelial lysyl oxidase induction by fibroblast-derived TNF-α. J Allergy Clin Immunol. 2019;144(1):171-82. Epub 20181220. doi: 10.1016/j.jaci.2018.10.067. PubMed PMID: 30578874; PMCID: PMC6586527.

50. Muir AB, Dods K, Noah Y, Toltzis S, Chandramouleeswaran PM, Lee A, Benitez A, Bedenbaugh A, Falk GW, Wells RG, Nakagawa H, Wang ML. Esophageal epithelial cells acquire functional characteristics of activated myofibroblasts after undergoing an epithelial to mesenchymal transition. Exp Cell Res. 2015;330(1):102-10. Epub 20140827. doi: 10.1016/j.yexcr.2014.08.026. PubMed PMID: 25183431; PMCID: PMC4489692.

51. Klochkova A, Fuller AD, Miller R, Karami AL, Panchani SR, Natarajan S, Mu A, Jackson JL, Klein-Szanto AJ, Muir AB, Whelan KA. A role for age-associated alterations in esophageal epithelium in eosinophilic esophagitis-associated fibrosis. Front Allergy. 2022;3:983412. Epub 20221215. doi: 10.3389/falgy.2022.983412. PubMed PMID: 36591561; PMCID: PMC9798296.

52. Valerio A, Cardile A, Cozzi V, Bracale R, Tedesco L, Pisconti A, Palomba L, Cantoni O, Clementi E, Moncada S, Carruba MO, Nisoli E. TNF-alpha downregulates eNOS expression and mitochondrial biogenesis in fat and muscle of obese rodents. J Clin Invest. 2006;116(10):2791-8. Epub 20060914. doi: 10.1172/JCI28570. PubMed PMID: 16981010; PMCID: PMC1564431.

53. Macias E, Rao D, Carbajal S, Kiguchi K, DiGiovanni J. Stat3 binds to mtDNA and regulates mitochondrial gene expression in keratinocytes. J Invest Dermatol. 2014;134(7):1971-80. Epub 20140204. doi: 10.1038/jid.2014.68. PubMed PMID: 24496235; PMCID: PMC4057971.
54. Yang S, He X, Zhao J, Wang D, Guo S, Gao T, Wang G, Jin C, Yan Z, Wang N, Wang Y, Zhao Y, Xing J, Huang Q. Mitochondrial transcription factor A plays opposite roles in the initiation and progression of colitis-associated cancer. Cancer Commun (Lond). 2021;41(8):695-714. Epub 20210623. doi: 10.1002/cac2.12184. PubMed PMID: 34160895; PMCID: PMC8360642.
55. Zhang X, Cheng E, Huo X, Yu C, Zhang Q, Pham TH, Wang DH, Spechler SJ, Souza RF. Omeprazole blocks STAT6 binding to the eotaxin-3 promoter in eosinophilic esophagitis cells. PLoS One. 2012;7(11):e50037. Epub 20121121. doi: 10.1371/journal.pone.0050037. PubMed PMID: 23185525; PMCID: PMC3503709.
56. Miller DE, Forney C, Rochman M, Cranert S, Habel J, Rymer J, Lynch A, Schroeder C, Lee J, Sauder A, Smith Q, Chawla M, Trimarchi MP, Lu X, Fjellman E, Brusilovsky M, Barski A, Waggoner S, Weirauch MT, Rothenberg ME, Kottyan LC. Genetic, Inflammatory, and Epithelial Cell Differentiation Factors Control Expression of Human Calpain-14. G3 (Bethesda). 2019;9(3):729-36. Epub 20190307. doi: 10.1534/g3.118.200901. PubMed PMID: 30626591; PMCID: PMC6404614.
57. Khan R, Lee JE, Yang YM, Liang FX, Sehgal PB. Live-cell imaging of the association of STAT6-GFP with mitochondria. PLoS One. 2013;8(1):e55426. Epub 20130130. doi: 10.1371/journal.pone.0055426. PubMed PMID: 23383189; PMCID: PMC3559584.
58. Kim H, Park SJ, Jou I. STAT6 in mitochondrial outer membrane impairs mitochondrial fusion by inhibiting MFN2 dimerization. iScience. 2022;25(9):104923. Epub 20220813. doi: 10.1016/j.isci.2022.104923. PubMed PMID: 36065189; PMCID: PMC9440285.
59. Zhu M, Min S, Mao X, Zhou Y, Zhang Y, Li W, Li L, Wu L, Cong X, Yu G. Interleukin-13 promotes cellular senescence through inducing mitochondrial dysfunction in IgG4-related sialadenitis. Int J Oral Sci. 2022;14(1):29. Epub 20220620. doi: 10.1038/s41368-022-00180-6. PubMed PMID: 35718799; PMCID: PMC9207030.
60. Vats D, Mukundan L, Odegaard JI, Zhang L, Smith KL, Morel CR, Wagner RA, Greaves DR, Murray PJ, Chawla A. Oxidative metabolism and PGC-1beta attenuate macrophage-mediated inflammation. Cell Metab. 2006;4(1):13-24. doi: 10.1016/j.cmet.2006.05.011. PubMed PMID: 16814729; PMCID: PMC1904486.
61. Scott O, Sharfe N, Dadi H, Vong L, Garkaby J, Abrego Fuentes L, Willett Pachul J, Nelles S, Nahum A, Roifman CM. Case Report: Eosinophilic Esophagitis in a Patient With a Novel STAT1 Gain-of-Function Pathogenic Variant. Front Immunol. 2022;13:801832. Epub 20220120. doi: 10.3389/fimmu.2022.801832. PubMed PMID: 35126392; PMCID: PMC8812721.
62. Bourke LT, Knight RA, Latchman DS, Stephanou A, McCormick J. Signal transducer and activator of transcription-1 localizes to the mitochondria and modulates mitophagy. JAKSTAT. 2013;2(4):e25666. Epub 20130715. doi: 10.4161/jkst.25666. PubMed PMID: 24470977; PMCID: PMC3902047.
63. Kaymak T, Kaya B, Wuggenig P, Nuciforo S, Göldi A, Oswald F, Roux J, Noti M, Melhem H, Hruz P, Niess JH, (SEECS) SECSG. IL-20 subfamily cytokines impair the

oesophageal epithelial barrier by diminishing filaggrin in eosinophilic oesophagitis. Gut. 2022. Epub 20220525. doi: 10.1136/gutjnl-2022-327166. PubMed PMID: 35613844.

64. Fu Z, Ye J, Dean JW, Bostick JW, Weinberg SE, Xiong L, Oliff KN, Chen ZE, Avram D, Chandel NS, Zhou L. Requirement of Mitochondrial Transcription Factor A in Tissue-Resident Regulatory T Cell Maintenance and Function. Cell Rep. 2019;28(1):159-71.e4. doi: 10.1016/j.celrep.2019.06.024. PubMed PMID: 31269437; PMCID: PMC6679941.

65. Dai XG, Li T, Huang WB, Zeng ZH, Li Q, Yang Y, Duan ZP, Wang YJ, Ai YH. Upregulation of Mitochondrial Transcription Factor A Promotes the Repairment of Renal Tubular Epithelial Cells in Sepsis by Inhibiting Reactive Oxygen Species-Mediated Toll-Like Receptor 4/p38MAPK Signaling. Pathobiology. 2019;86(5-6):263-73. Epub 20190820. doi: 10.1159/000501789. PubMed PMID: 31430762.

66. Woo DK, Green PD, Santos JH, D'Souza AD, Walther Z, Martin WD, Christian BE, Chandel NS, Shadel GS. Mitochondrial genome instability and ROS enhance intestinal tumorigenesis in APC(Min/+) mice. Am J Pathol. 2012;180(1):24-31. Epub 20111103. doi: 10.1016/j.ajpath.2011.10.003. PubMed PMID: 22056359; PMCID: PMC3338350.

67. Balliet RM, Capparelli C, Guido C, Pestell TG, Martinez-Outschoorn UE, Lin Z, Whitaker-Menezes D, Chiavarina B, Pestell RG, Howell A, Sotgia F, Lisanti MP. Mitochondrial oxidative stress in cancer-associated fibroblasts drives lactate production, promoting breast cancer tumor growth: understanding the aging and cancer connection. Cell Cycle. 2011;10(23):4065-73. Epub 20111201. doi: 10.4161/cc.10.23.18254. PubMed PMID: 22129993; PMCID: PMC3272288.

68. Hamanaka RB, Glasauer A, Hoover P, Yang S, Blatt H, Mullen AR, Getsios S, Gottardi CJ, DeBerardinis RJ, Lavker RM, Chandel NS. Mitochondrial reactive oxygen species promote epidermal differentiation and hair follicle development. Sci Signal. 2013;6(261):ra8. Epub 20130205. doi: 10.1126/scisignal.2003638. PubMed PMID: 23386745; PMCID: PMC4017376.

69. Vander Heiden MG, Cantley LC, Thompson CB. Understanding the Warburg effect: the metabolic requirements of cell proliferation. Science. 2009;324(5930):1029-33. doi: 10.1126/science.1160809. PubMed PMID: 19460998; PMCID: PMC2849637.

70. Reyes Hueros RA, Gier RA, Shaffer SM. Non-genetic differences underlie variability in proliferation among esophageal epithelial clones. PLoS Comput Biol. 2024;20(10):e1012360. Epub 20241028. doi: 10.1371/journal.pcbi.1012360. PubMed PMID: 39466790; PMCID: PMC11573201.

71. Fuller AD, Karami AL, Kabir MF, Klochkova A, Jackson JL, Mu A, Tan Y, Klein-Szanto AJ, Whelan KA. Eosinophilic esophagitis-associated epithelial remodeling may limit esophageal carcinogenesis. Front Allergy. 2023;4:1086032. Epub 20230329. doi: 10.3389/falgy.2023.1086032. PubMed PMID: 37064719; PMCID: PMC10090679.

72. Clevenger MH, Karami AL, Carlson DA, Kahrilas PJ, Gonsalves N, Pandolfino JE, Winter DR, Whelan KA, Tétreault MP. Suprabasal cells retain progenitor cell identity programs in eosinophilic esophagitis-driven basal cell hyperplasia. JCI Insight. 2023;8(19). Epub 20231009. doi: 10.1172/jci.insight.171765. PubMed PMID: 37672481; PMCID: PMC10619442.

Figure 1. Evidence of increased mitochondria in EoE patients. (**A**) Representative images of immunohistochemistry (IHC) staining for mitochondrially-encoded cytochrome oxidase 1 (MTCO1) in esophageal biopsies from human subjects classified as normal, active EoE or inactive EoE. Scale bars, 50 μm. (**B**) Average MTCO1 score in esophageal epithelium of indicated groups. Data in bar graphs presented as mean ± SEM. *p<0.05; **p<0.01.

Figure 2. Evidence of increased mitochondria in esophageal epithelium of mice with EoE-like inflammation. C57B6 mice were treated with MC903 and Ovalbumin (OVA) over 32-days then esophagi were dissected, and epithelium was peeled. MC903-only treated mice served as controls. (**A**) Immunoblotting for MTCO1 protein expression with Actin as a loading control. (**B**) Quantitative PCR (qPCR) was used to assess mtDNA levels with *Ikbβ* as an internal control. Data in bar graphs presented as mean ± SEM. *p<0.05; n=7 for MC903-only controls and n=7 for MC903+/OVA+.

Figure 3. Effects of EoE-relevant cytokines on mitochondria in human esophageal keratinocytes *in vitro*. (**A**) EPC2-hTERT cells were treated with the indicated cytokines for 7 days. All interleukin (IL) treatments were at a final concentration of 10 ng/mL. Tumor necrosis factor (TNF)α treatment was at a final concentration of 40 ng/mL. qPCR evaluated levels of mitochondrially-encoded genes *MTCO1* and *ND6*, and nuclear-encoded gene *COXIV*. All genes are shown normalized to *GAPDH*. (**B, C**) EPC2-hTERT and primary esophageal epithelial cultures were treated with IL-13 (10 ng/mL) for 7 days then stained with MitoTracker Green and Hoechst 33342 to visualize mitochondria and nuclei, respectively, using confocal microscopy. (**B**) Representative images are shown. (**C**) Quantitative fluorescence intensity of MitoTracker Green-stained EPC2-hTERT cells

was analyzed by ImageJ software. Data in bar graphs presented as mean ± SEM, *p<0.05; n=3.

Figure 4. Effects of IL-13 and IL-4 on mediators of mitochondrial dynamics in esophageal keratinocytes. (**A-F**) EPC2-hTERT cells were treated with IL-13 (10 ng/mL) for the noted time points. Relative expression of (**A**) *TFAM,* (**B**) *MFN1,* (**C**) *MFN2,* (**D**) *DPR1,* (**E**) *PINK1,* and (**F**) *PARK2* was determined by qPCR. (**G, H**) Western blot showing for TFAM in EPC2-hTERT cells after 7 days of treatment with 10 ng/mL IL-13 (**G**) or IL-4 (**H**) with Actin as a loading control. (**I**) RNA expression of *TFAM, MFN1, MFN2, PINK1,* and *PARK2* expression in esophageal epithelium of active EoE patients and normal controls using data from Sherrill et al[36]. qPCR data was normalized to β-actin. Data in bar graphs presented as mean ± SEM, *p<0.05; **p<0.01; ***p<0.001; n=3.

Figure 5. Effects of JAK inhibitor ruxolitinib on IL-13- and IL-4-mediated mitochondrial biogenesis in esophageal keratinocytes. EPC2-hTERT cells were treated with 10 ng/mL IL-13 or IL-4 for 7 days in the presence or absence of JAK inhibitor Ruxolitinib (100 ng/mL). (**A**) Immunoblotting was used to assess expression of indicated proteins, including STAT6 phosphorylated tyrosine (Y) residue 641. Actin serves as a loading control. (**B**) Levels of mtDNA-encoded genes *MTCO1* and *ND6*, and nuclear-encoded gene *COXIV* were evaluated by qPCR. Data in bar graphs presented as mean ± SEM. *p<0.05; n=3.

Figure 6. Effects of genetic depletion of TFAM on IL-13-mediated impairment of squamous cell differentiation in 3D organoids. (**A**) Schematic outlining approach for testing effects of Cre-mediated depletion of TFAM in organoids generated from esophageal epithelium of *Tfam*$^{loxp/loxp}$ mice. Adenoviral Cre and IL-13 (10 ng/mL) was added to organoids at the time of plating. After 7 days of growth, organoids were fixed and paraffin embedded. (**B**) Morphology of esophageal organoids was assessed via Hematoxylin & Eosin (H&E) staining and TFAM expression was assessed by IHC.

Figure 7. Effects of IL-13 on mitochondrial respiration, ATP level, and mitochondrial depolarization in esophageal keratinocytes. Esophageal epithelial cells were treated with IL-13 (10 ng/mL) for 7 days. (**A-D**) In EPC2-hTERT cells, mitochondrial bioenergetics was assessed by Seahorse respirometry. Specific parameters determined were (**A**) oxygen consumption rate; (**B**) basal respiration; (**C**) ATP-linked respiration; and (**D**) maximal respiration. (**E-G**) Relative ATP measurement by ATP determination assay in (**E**) EPC2-hTERT cells; (**F**) normal primary esophageal keratinocytes; (**G**) and (**G**) primary esophageal keratinocytes derived from patient with active EoE. (**H, I**) MitoTracker Red/Green flow cytometry was performed in EPC2-hTERT cells. (**H**) Representative flow cytometry dot plots. (**I**) Bar diagram showing

percentage of cells with depolarized mitochondria. Data in bar graphs presented as mean ± SEM. *p<0.05; **p<0.01; ***p<0.001; ****p<0.0001; n=3.

Figure 8. Effects of TFAM depletion on IL-13-mediated suppression of mitochondrial reactive oxygen species. (**A, B**) EPC2-hTERT cells were treated with 10 ng/mL IL-13 for 7 days then stained with MitoSOX fluorescence and assessed by flow cytometry. (A)of IL-13-treated EPC2-hTERT cells with mean fluorescent intensity bar graph. (**A**) Representative flow histograms and (**B**) bar diagram showing average mean fluorescence intensity are shown. (**C, D**) EPC2-hTERT cells were transfected with siRNA targeting TFAM (siTFAM) or non-targeting (siNT) control oligonucleotides for 72 hours. Cells were then cultured in the presence or absence of IL-13 (10 ng/µl) for 7 days and stained with MitoSOX Red and Hoechst 33342 to assess superoxide and nuclei, respectively, by confocal imaging. (**C**) Representative confocal images and (**D**) bar diagram quantifying relative fluorescence are shown. Data in bar graphs presented as mean ± SEM. **p<0.01; ***p<0.001; ****p<0.0001; n=3.

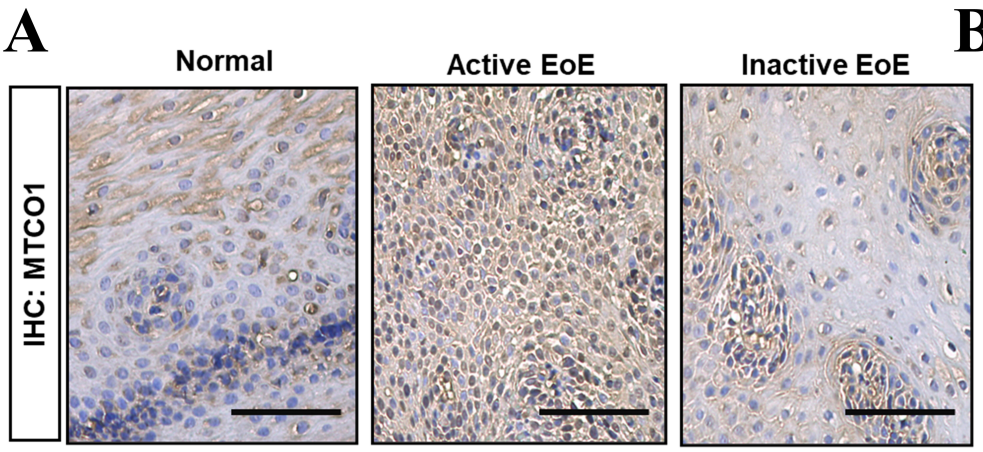
A
Normal
Active EoE
Inactive EoE
IHC: MTCO1

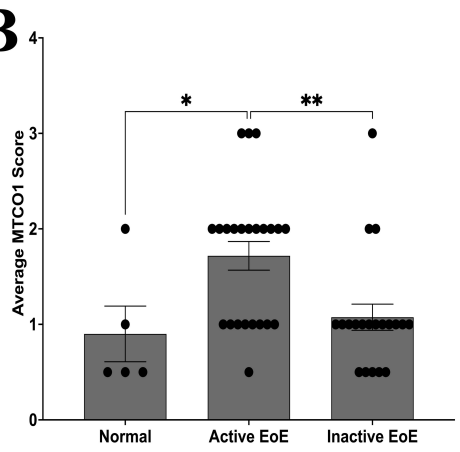
B
Average MTCO1 Score
0
1
2
3
4
*
**
Normal
Active EoE
Inactive EoE

Figure 1

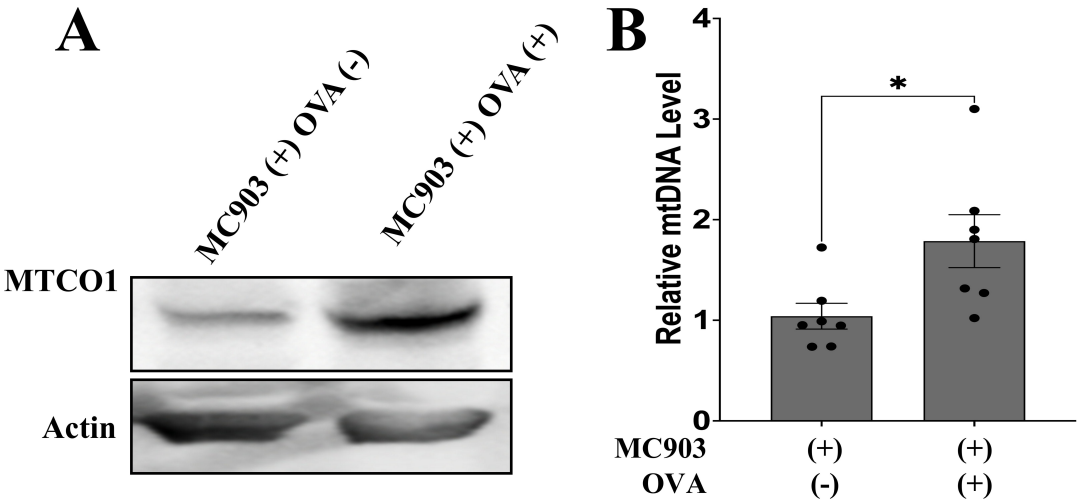
A
MC903 (+) OVA (-)
MC903 (+) OVA (+)
MTCO1
Actin
B
Relative mtDNA Level
4
3
2
1
0
*
MC903
OVA
(+)
(-)
(+)
(+)

Figure 2

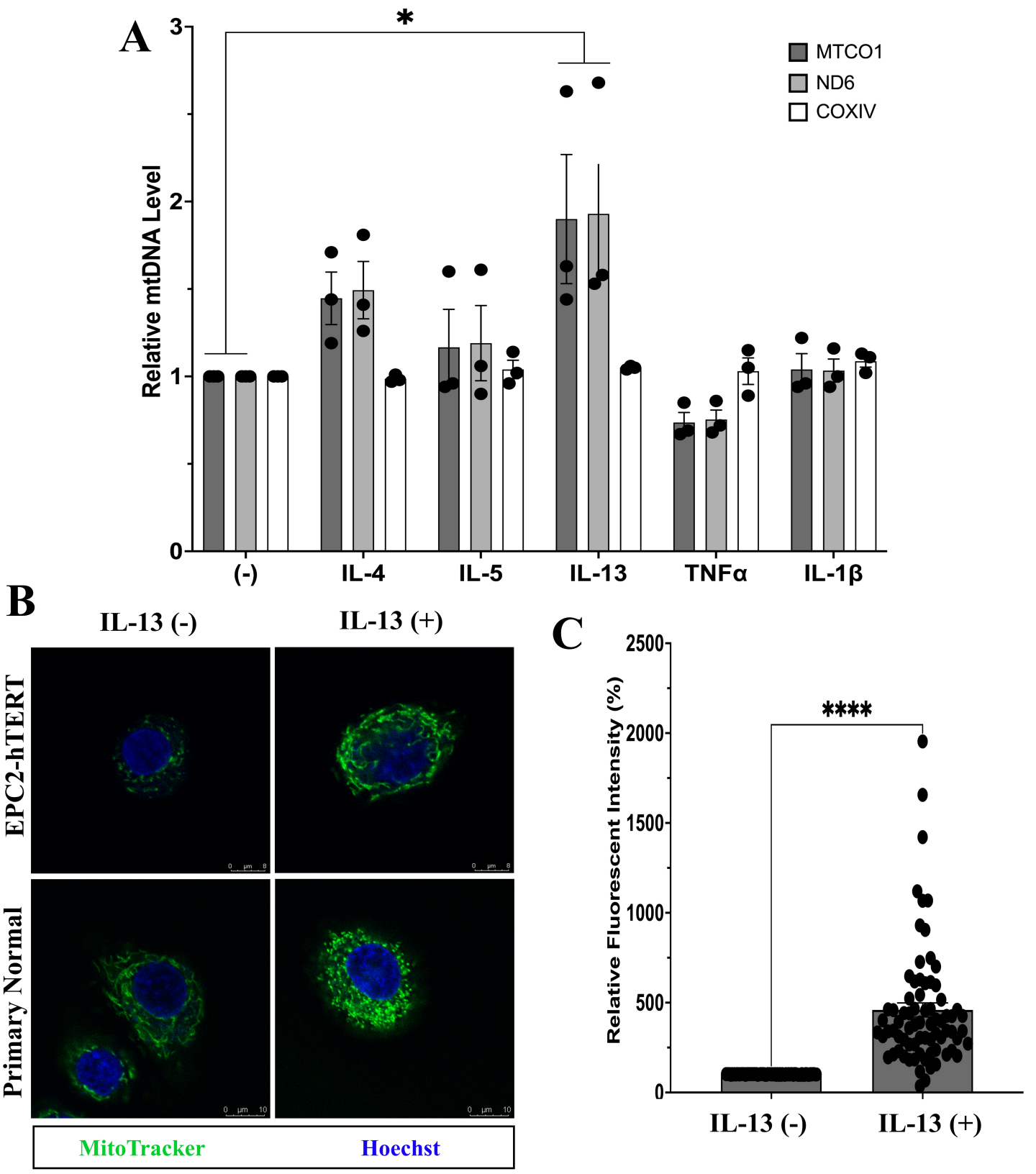
A
*
MTCO1
ND6
COXIV
Relative mtDNA Level
3
2
1
0
(-)
IL-4
IL-5
IL-13
TNFα
IL-1β
B
IL-13 (-)
IL-13 (+)
EPC2-hTERT
Primary Normal
MitoTracker
Hoechst
C
****
Relative Fluorescent Intensity (%)
2500
2000
1500
1000
500
0
IL-13 (-)
IL-13 (+)

Figure 3

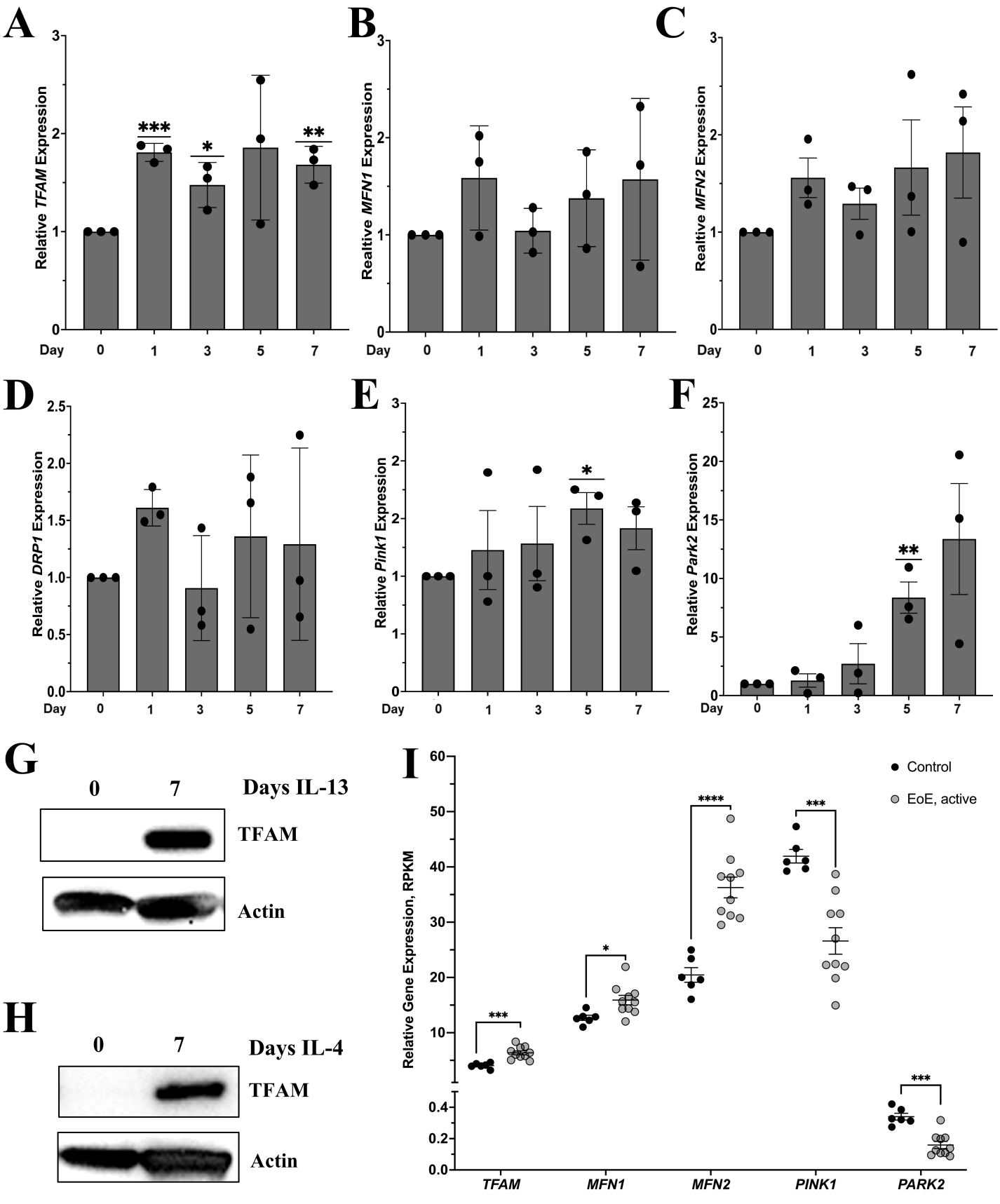
A
Relative TFAM Expression
***
*
**
Day 0 1 3 5 7
B
Realtive MFN1 Expression
Day 0 1 3 5 7
C
Realtive MFN2 Expression
Day 0 1 3 5 7
D
Relative DRP1 Expression
Day 0 1 3 5 7
E
Relative Pink1 Expression
*
Day 0 1 3 5 7
F
Relative Park2 Expression
**
Day 0 1 3 5 7
G
0 7 Days IL-13
TFAM
Actin
H
0 7 Days IL-4
TFAM
Actin
I
Control
EoE, active
Relative Gene Expression, RPKM
***
*
****
***
***
TFAM MFN1 MFN2 PINK1 PARK2

Figure 4

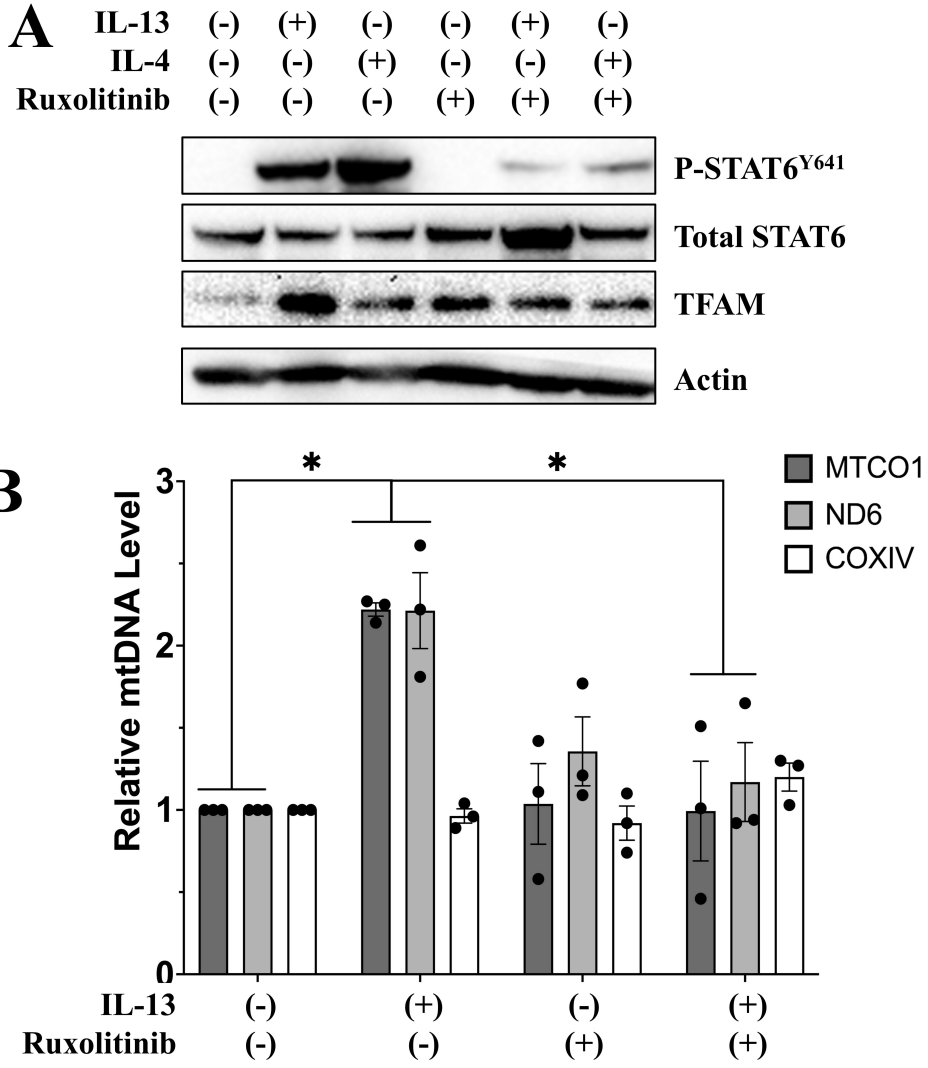
A
IL-13 (-) (+) (-) (-) (+) (-)
IL-4 (-) (-) (+) (-) (-) (+)
Ruxolitinib (-) (-) (-) (+) (+) (+)
P-STAT6Y641
Total STAT6
TFAM
Actin
B
Relative mtDNA Level
0
1
2
3
*
*
MTCO1
ND6
COXIV
IL-13 (-) (+) (-) (+)
Ruxolitinib (-) (-) (+) (+)

Figure 5

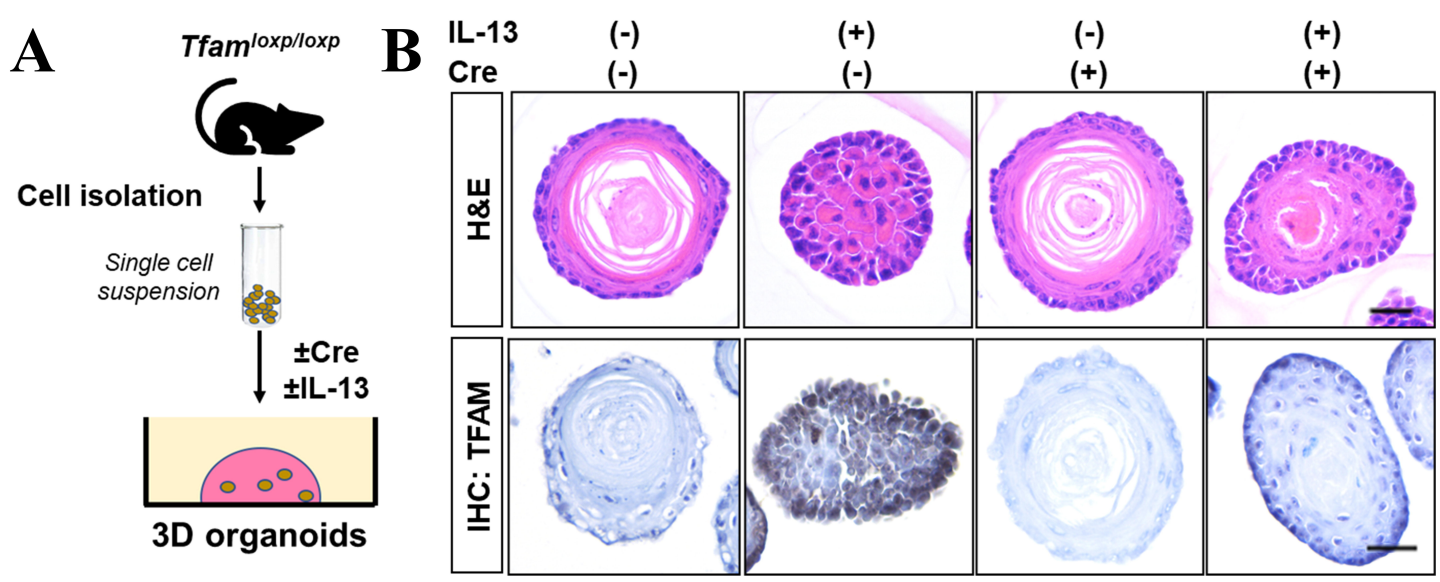
A
Tfam loxp/loxp
Cell isolation
Single cell suspension
±Cre
±IL-13
3D organoids
B
IL-13 (-) (+) (-) (+)
Cre (-) (-) (+) (+)
H&E
IHC: TFAM

Figure 6

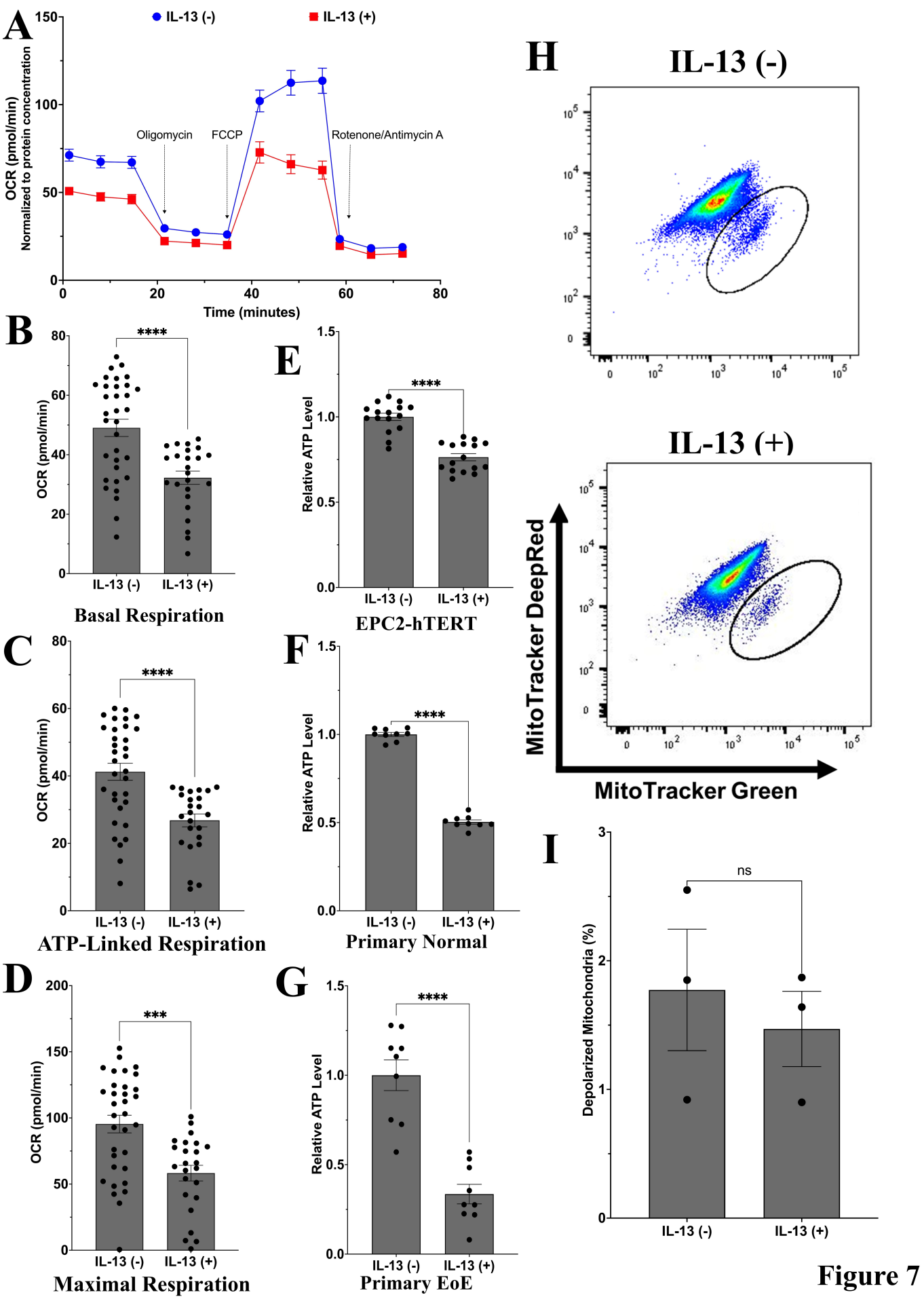
A
IL-13 (-)
IL-13 (+)
OCR (pmol/min)
Normalized to protein concentration
Oligomycin
FCCP
Rotenone/Antimycin A
Time (minutes)
B
OCR (pmol/min)
****
IL-13 (-)
IL-13 (+)
Basal Respiration
C
OCR (pmol/min)
****
ATP-Linked Respiration
D
OCR (pmol/min)
***
Maximal Respiration
E
Relative ATP Level
****
EPC2-hTERT
F
Relative ATP Level
****
Primary Normal
G
Relative ATP Level
****
Primary EoE
H
IL-13 (-)
IL-13 (+)
MitoTracker DeepRed
MitoTracker Green
I
Depolarized Mitochondria (%)
ns

Figure 7

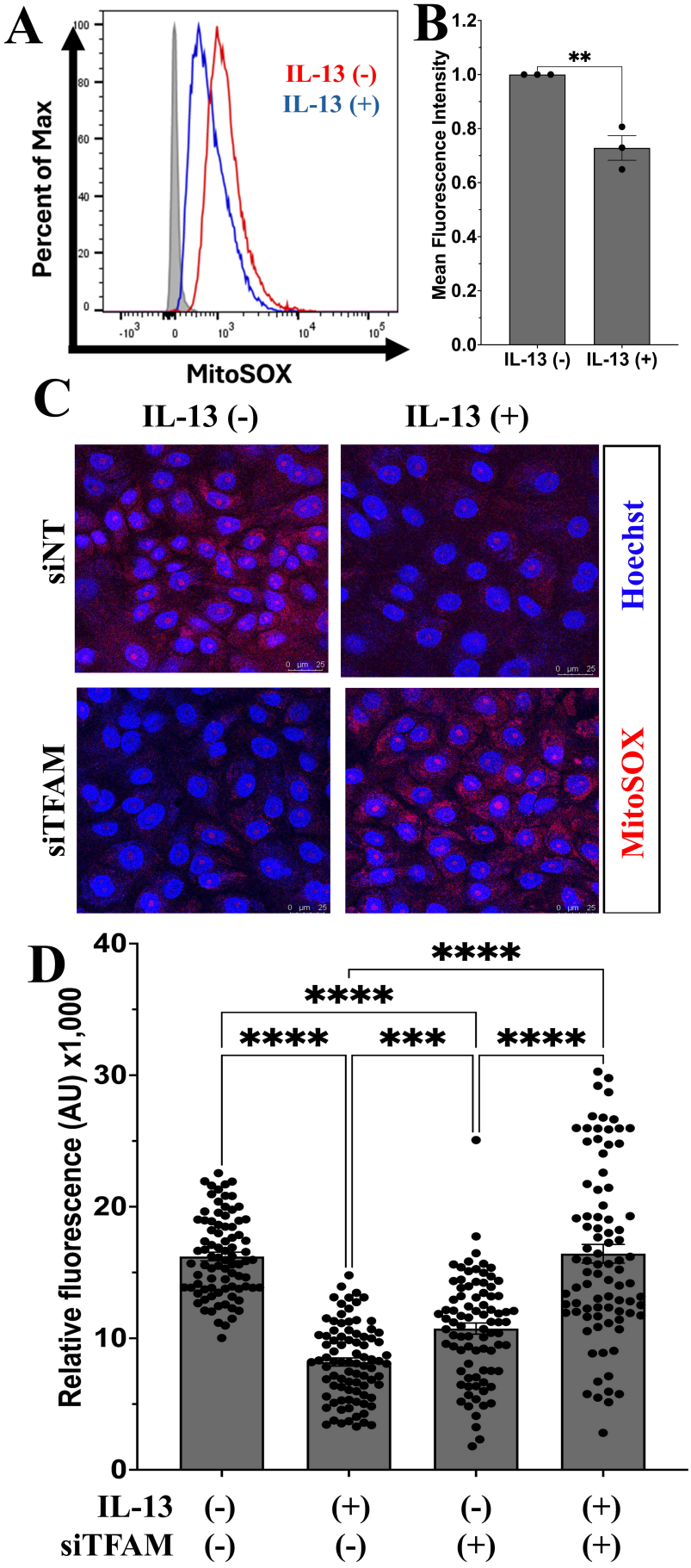
A
Percent of Max
MitoSOX
IL-13 (-)
IL-13 (+)
B
Mean Fluorescence Intensity
**
IL-13 (-)
IL-13 (+)
C
IL-13 (-)
IL-13 (+)
siNT
siTFAM
Hoechst
MitoSOX
D
Relative fluorescence (AU) x1,000
****
****
****
***
****
IL-13 (-) (+) (-) (+)
siTFAM (-) (-) (+) (+)

Figure 8